The age of reason: Functional brain network development during childhood

Ursula A. Tooley[1,2], Anne T. Park[1], Julia A. Leonard[3], Austin L. Boroshok[1], Cassidy L. McDermott[1], M. Dylan Tisdall[4], Dani S. Bassett[5,6,7,8,9,10], & Allyson P. Mackey[1]

Created 2022-07-07

Affiliations

[1] Department of Psychology, School of Arts and Sciences, University of Pennsylvania, Philadelphia, PA 19104, USA

[2] Neuroscience Graduate Group, Perelman School of Medicine, University of Pennsylvania, Philadelphia, PA 19104, USA

[3] Department of Psychology, Yale University, New Haven, CT 06520, USA

[4] Department of Radiology, Perelman School of Medicine, University of Pennsylvania, Philadelphia, PA, 19104

[5] Department of Bioengineering, School of Engineering and Applied Sciences, University of Pennsylvania, Philadelphia, PA 19104, USA

[6] Department of Electrical & Systems Engineering, School of Engineering and Applied Science, University of Pennsylvania, Philadelphia, PA 19104, USA

[7] Department of Physics & Astronomy, School of Arts and Sciences, University of Pennsylvania, Philadelphia, PA 19104, USA

[8] Department of Neurology, Perelman School of Medicine, University of Pennsylvania, Philadelphia, PA 19104, USA

[9] Department of Psychiatry, Perelman School of Medicine, University of Pennsylvania, Philadelphia, PA 19104, USA

[10] Santa Fe Institute, Santa Fe, NM 87501 USA

Corresponding author: mackeya@upenn.edu

Abstract

Human childhood is characterized by dramatic changes in the mind and brain. However, little is known about the large-scale intrinsic cortical network changes that occur during childhood due to methodological challenges in scanning young children. Here, we overcome this barrier by using sophisticated acquisition and analysis tools to investigate functional network development in children between the ages of 4 and 10 years ($n = 92$). At multiple spatial scales, age is positively associated with brain network segregation. At the system level, age was associated with segregation of systems involved in attention from those involved in abstract cognition, and with integration among attentional and perceptual systems. Associations between age and functional connectivity are most pronounced in visual and medial prefrontal cortex, the two ends of a gradient from perceptual, externally oriented cortex to abstract, internally oriented cortex. These findings suggest that both ends of the sensory-association gradient may develop early, in contrast to the classical theories that cortical maturation proceeds from back to front, with sensory areas developing first and association areas developing last. More mature patterns of brain network architecture, controlling for age, were associated with better visuospatial reasoning abilities. Our results suggest that as cortical architecture becomes more specialized, children become more able to reason about the world and their place in it.

Keywords: childhood, functional network, development, graph theory, reasoning

Significance

Anthropologists have called the transition from early to middle childhood the "age of reason", when children across cultures become more independent. We employ cutting-edge neuroimaging acquisition and analysis approaches to investigate associations between age and functional brain architecture in childhood. Age was positively associated with segregation between cortical systems that process the external world, and those that process abstract phenomena like the past, future, and minds of others. Surprisingly, we observed pronounced development at both ends of the sensory-association gradient, challenging the theory that sensory areas develop first and association areas develop last. Our results open new directions for research into how brains

1 reorganize to support rapid gains in cognitive and socioemotional skills as children reach the age
2 of reason.

Introduction

4 Children's minds develop fastest during the first decade of life. Sensory and motor skills develop
5 before complex cognitive skills: children can see and walk before they can solve abstract puzzles.
6 Diverse skills including reasoning, executive function, emotion regulation, and social cognition all
7 improve dramatically until 8-10 years of age, after which change slows down (see Akshoomoff et
8 al. (2014); Kopp (1989); Wellman (2014); Whitaker et al. (2018); but see also Fortenbaugh et al.
9 (2015)). Developmental psychologists once called these changes the "5-to-7-year shift": the
10 transition from Piaget's preoperational stage, in which children rely on perceptual information, to
11 the concrete operational stage, in which children are less bound by perceptual information and
12 more able to think abstractly (Sameroff and Haith, 1996). Anthropologists have called this
13 developmental period the "age of reason" or the "age of sense", when children become more
14 independent from their parents, begin to build more complex social relationships with peers and
15 other adults, and become less egocentric and more able to understand others' perspectives
16 (Chandler and Lalonde, 1996; Lancy, 2014).

17 A core tenet of developmental cognitive neuroscience is that brain development proceeds along
18 the sensory-association axis, with sensory areas developing first and association areas developing
19 last (Sydnor et al., 2021; Tooley et al., 2021). This sequence is in line with data from both
20 behavioral and cognitive development (Cole et al., 2005). The far end of the association axis is
21 anchored by the default mode system (Smallwood et al., 2021), which is furthest from sensory
22 input and engages primarily in abstract cognitive processes that do not rely on the current
23 sensory environment. Examples of such processes include remembering the past, projecting the
24 future, and taking the perspective of others (Buckner and DiNicola, 2019). Other association
25 systems, such as the dorsal and ventral attention systems, receive and process more input from
26 the outside world (Corbetta and Shulman, 2002). The frontoparietal system can be thought of as a
27 toggle controlling the switch between internally and externally oriented cognition, flexibly
28 coordinating other systems and holding sensory information online. Such processes are commonly
29 exemplified in working memory and reasoning tasks (Owen et al., 2005; Cole et al., 2013).

1   Data on structural brain development, including cortical thinning, surface area, and white matter

2   coherence, clearly support early development of sensory areas (Stiles and Jernigan, 2010;

3   Raznahan et al., 2011; Whitaker et al., 2016; Gennatas et al., 2017; Reynolds et al., 2019). However,

4   regions of the default mode system, including the medial prefrontal cortex and the precuneus, also

5   show early structural development (Brown and Jernigan, 2012; Li et al., 2013; Wierenga et al.,

6   2014; Li et al., 2015). Thus, another possibility is that both ends of the sensory-association axis

7   become anchored early in life, and developmental processes differentiate and refine the

8   boundaries of attention and executive systems along this axis later in development. Brain

9   structure is easier to measure than function in sleeping children, so it has been better

10 characterized in early childhood (see Houston et al. (2014) and Lenroot and Giedd (2006)).

11 However, brain function may be more closely linked to cognition and behavior (Zimmermann et

12 al., 2018; Dhamala et al., 2021), particularly during development when the brain is highly plastic

13 (Chen et al., 2020).

14 Functional brain networks can be studied at multiple spatial scales: in the whole brain, across

15 systems, and among regions or parcels. Understanding how functional networks reorganize at the

16 whole brain level allows us to examine the extent to which segregation is an overall guiding

17 principle of development, while studying the constituent systems (sometimes referred to as

18 "networks" in the literature) allows for examination of relationships among specialized functional

19 subnetworks. The parcel resolution yields more granular detail about which specific brain areas,

20 or network nodes, might drive effects. Segregation refers to the presence of groups or

21 subnetworks of densely interconnected nodes, and is thought to emerge partially as a result of

22 maturing inhibitory interneurons; synchronized inhibition may be necessary for establishing

23 segregated network function (Cardin, 2018; Kraft et al., 2020; Chini et al., 2021).

24 Functional network development has been studied predominantly in middle childhood (7-10

25 years) or later (see Morgan et al. (2018) and Grayson and Fair (2017) for review), due to the

26 challenges of acquiring high quality data in younger children while they are awake. From middle

27 childhood through adolescence, at the whole brain level, networks become more modular and

28 segregated with age, supporting improved cognition (Satterthwaite et al., 2013b; Gu et al., 2015;

29 Grayson and Fair, 2017; Marek et al., 2019). At the system resolution, age is associated with

30 increases in within-system connectivity, and decreases in between-system connectivity,

1   particularly between the default mode system and executive control and attention systems (Fair et

2   al., 2008; Chai et al., 2013; Satterthwaite et al., 2013b; Gu et al., 2015; Lopez et al., 2019; Jones et

3   al., 2021). At the regional level, effects are less consistent, perhaps because findings vary widely

4   depending on the age range studied (Grayson and Fair, 2017; Morgan et al., 2018). Another way to

5   examine parcel-level effects is to examine the development of the sensory-association axis across

6   cortex. Two recent and well-powered studies found that in middle childhood, a sensory-

7   association gradient is in place, but the most variance in patterns of connectivity is explained by

8   separation between visual and somatomotor systems (Dong et al., 2021; Xia et al., 2022). By age

9   12 years, however, the organization of the sensory-association gradient resembles that of adults;

10   development of the primary sensory-association gradient may be mediated by changes in network

11   architecture (Dong et al., 2021; Xia et al., 2022). Functional network architecture has been shown

12   to have cognitive consequences: youth with more segregated networks, and in particular task-

13   positive (i.e., attention and control systems) and task-negative (i.e., default mode) systems,

14   perform better on a wide variety of cognitive tasks (Gu et al., 2015; Lopez et al., 2019; Marek et al.,

15   2019; Jones et al., 2021; Xia et al., 2022).

16   A few studies have characterized functional network development in children younger than 6

17   years of age, and overall suggest developmental specialization of cortex with age. *In utero*, a proto-

18   default-mode system is detectable, and visual and motor systems show overlap with that found in

19   adults, but attention and frontoparietal systems remain undifferentiated (Turk et al., 2019;

20   Thomason, 2020). Infant brain networks can be studied during sleep: primary sensory systems

21   have an adult-like architecture at birth, but default, ventral attention, and dorsal attention systems

22   do not develop a distributed network architecture until 1-2 years of age, and executive control

23   systems are still immature at 2 years of age (Gilmore et al., 2018). The anticorrelation between

24   default and dorsal attention system connectivity begins to emerge around 1 year of age (see Gao et

25   al. (2013), $n = 147$). From the age of 3 months to 6 years, within-system connectivity broadly

26   increases with age, while between-system connectivity decreases (see Bruchhage et al. (2020),

27    $n = 196$, natural sleep). Another way to address challenges involved in scanning young children is

28   to have them view movies: a study of children aged 4 to 7 years showed that age was positively

29   associated with connectivity in systems identified with an independent component analysis,

30   including sensory, motor, default mode, and executive control systems, but not the ventral

5

attention system (see Rohr et al. (2018), $n = 60$). An analysis of the same sample also found that age was negatively associated with connectivity between seeds in the dorsal attention system (intraparietal sulcus, frontal eye fields) and areas of the default mode system (Rohr et al. (2017), $n = 44$). In general, more mature patterns of connectivity are associated with better performance on measures of attention and cognition (Rohr et al., 2017, 2018; Bruchhage et al., 2020; Qi et al., 2021). These studies of young children have examined connectivity between specific regions or subsets of regions, but not the architecture of intrinsic cortical networks at rest. Hence, little is known about how rewiring of intrinsic functional networks supports the profound cognitive changes that take place during childhood.

The present research

Here we focused on functional brain network development between the ages of 4 and 10 years ($n = 92$). To overcome barriers associated with resting-state data collection from young children, we applied sophisticated neuroimaging acquisition and analysis approaches to minimize motion and its impacts, including sequences optimized to reduce motion artifacts (Tisdall et al., 2012), real-time motion monitoring (Dosenbach et al., 2017), rigorous image quality assurance using open-source tools, and a preprocessing pipeline optimized to reduce the impact of head motion. We used network science tools to take a hierarchical analytical approach, asking first whether whole-brain measures of network topology are associated with age, and then which systems and parcels of cortex drive patterns of topological refinement. Finally, we asked whether network structure was associated with cognition. We focused on reasoning because it is a core skill that develops rapidly until middle childhood (Whitaker et al., 2018), is highly predictive of later academic outcomes (Fuchs et al., 2006; Ferrer et al., 2007; Pagani et al., 2017), and was assessed across the majority of our sample. If age-associated changes in network architecture support reasoning skills, then individual differences in reasoning, controlling for age, should mirror associations with age. In other words, we predict that children with more mature functional architecture, i.e., greater network segregation, should have better cognitive skills.

Materials & Methods

Participants

The Institutional Review Board at the University of Pennsylvania approved this study. All parents provided informed, written consent. Children younger than age 8 provided verbal assent, and children ages 8 and older provided written assent. Participants were recruited from Philadelphia and the surrounding regions through advertisements on public transportation, partnerships with local schools, outreach programs, community family events, and social media ads. Children were between the ages of 4 and 10.59 years ($M = 6.85$, $SD = 1.38$). We chose to collect data from children starting at 4 years of age, as collecting functional brain imaging data from awake children younger than 4 may result in large amounts of unusable data. Parents were asked to report their child's gender and were provided four sex categories: female, male, other, and prefer not to answer. We recognize that the wording of this question conflated sex and gender, making it impossible for us to investigate the relation between brain development and the child's gender identity, whether within or outside the binary. 54% of children were reported by parents to be male and 46% were reported by parents to be female; none were reported to be other, suggesting that we might not have any intersex children in our sample. The racial and ethnic makeup of the sample was as follows: 61% Black, 36% white, 20% Asian, 8% other, and 10% Hispanic/Latino. Percentages sum to greater than 100% because parents or guardians could endorse multiple races. 49% of children had a parent with a college degree or more education and 45% had an annual family income of $50,000 or more. For comparison, Philadelphia is 43.6 % Black, 44.8 % White, 7.8 % Asian, 3.9 % Other, and 15.2 % Hispanic or Latino, and the median household income was $49,127 (US Census Bureau, 2020).

The target sample size was 123 children with usable data to detect correlations of $r = .25$ with a power of greater than .8. However, data usability in young children can be difficult to predict, and data collection was cut short in 2020 by the COVID-19 pandemic. Resting-state scans were acquired for 138 participants. Ninety-two participants were included in the final sample. Participants were excluded for not completing the resting-state scan (e.g., due to falling asleep or wanting to end the scan early, $n = 17$), or parent-reported diagnosis of Attention-

1 Deficit/Hyperactivity Disorder or developmental delay during the visit, despite not reporting a

2 diagnosis during screening ($n = 4$).

3 To mitigate the effect of image quality on our analyses, we also employed motion and quality

4 exclusions, excluding children with average framewise displacement (FD) > 1 mm ($n = 14$), and

5 censored volumes at 0.5 mm FD. We further excluded children with > 30% of frames exceeding 0.5

6 mm FD ($n = 8$, Power et al. (2012)) or artifacts ($n = 3$, see below for details).These criteria were

7 selected to balance the need to include as much data as possible in a young population (Leonard et

8 al., 2017) and the need to limit the influence of low-quality on connectivity metrics (Power et al.,

9 2014a).

10 We conducted an additional sensitivity analysis with stricter motion cutoffs: excluding children

11 with > 0.5 mm average FD ($n = 9$) and censoring volumes with > 0.25 mm FD.

12 25 children were excluded for image artifacts or motion in the original sample. At the more lenient

13 threshold, these children were younger than the included children ($t(40.15) = -2.79, p = .008$),

14 but not different on age-normed reasoning scores ($t(37.60) = -1.47, p = .150$). At the stricter

15 threshold, 34 children were excluded for image artifacts or motion: excluded children were

16 younger than the included children ($t(50.96) = -2.13, p = .038$), but not different on age-normed

17 reasoning scores ($t(52.15) = -1.46, p = .150$).

18 ***Data acquisition***

19 Prior to the scanning session, participants were acclimated to the scanning environment with a

20 mock scanner that simulates typical MRI noises. Participants practiced keeping still in the mock

21 scanner, by watching a movie that would pause each time they moved their heads more than 1

22 mm. During the MRI session, a researcher stayed in the scanner room with the participant to

23 reassure the child. Participants viewed a fixation cross on a gray screen throughout the resting-

24 state scan.

25 Imaging was performed at the Center for Advanced Magnetic Resonance Imaging and

26 Spectroscopy (CAMRIS) at the University of Pennsylvania. Scanning was conducted using a

27 Siemens MAGNETOM Prisma 3 T MRI scanner with the vendor's 32-channel coil. 5-minute resting-

28 state fMRI scans were acquired using a T2*-weighted multiband gradient-echo echo-planar

imaging (EPI) sequence (TR = 2000 ms, TE = 30.2 ms, BW = 1860 Hz/px, flip angle = 90∘, voxel size = 2 mm isotropic, matrix size = 96 × 96, 75 axial slices, FOV = 192 mm, volumes = 150–240, 5 dummy scans, multiband acceleration factor = 3). We chose a multiband factor of 3 to minimize interactions between multiband and motion (Risk et al., 2021). A whole-brain, high-resolution, T1-weighted 3D-encoded multi-echo anatomical image (MEMPRAGE) was acquired (TR = 2530 ms, TEs = 1.69 ms/3.55 ms/5.41 ms/7.27 ms, BW =650 Hz/px, 3x GRAPPA, flip angle = 7∘, voxel size =1 mm isotropic, matrix size = 256 × 256, 176 sagittal slices, FOV =256 mm, total scan time of 4:38 minutes). This anatomical sequence used interleaved volumetric navigators to prospectively track and correct for subject head motion (Tisdall et al., 2012).

To increase the amount of usable data, midway through data collection, we updated our acquisition strategy in two ways: (i) monitoring head motion in real-time using the Framewise Integrated Real-time MRI Monitor (FIRMM) system (Dosenbach et al., 2017), and (ii) collecting 10 minutes of low-motion resting-state data (2 resting-state runs of data with FD < 1 mm) when possible. An incidental feature of this design choice is that it decouples age, and reasoning ability, from the amount of data acquired for each child. One scan was acquired for 43 children, two scans were acquired for 48 children, and three scans were acquired for one child. Participants were eligible for inclusion if they had more than 135 frames of resting-state data. Participants had an average FD of 0.3 mm ($SD = 0.18$ mm). For participants with more than one usable resting-state run, we took an average of FD across runs, weighted by run length. All analyses controlled for average FD and total number of resting-state frames collected.

Image preprocessing

Results included in this manuscript come from preprocessed data, where the preprocessing was performed using Freesurfer (Dale et al., 1999), fMRIPprep 1.2.6-1 (Esteban et al. (2018); Esteban et al. (2019); RRID:SCR_016216), which is based on Nipype 1.1.7 (Gorgolewski et al. (2017); Gorgolewski et al. (2011); RRID:SCR_002502), as well as xcpEngine 1.0 (Ciric et al., 2018). Brain surfaces were reconstructed using recon-all (Dale et al., 1999) prior to other processing, and reconstructed surfaces were used as input to fMRIprep.

The T1-weighted (T1w) image was corrected for intensity non-uniformity (INU) using N4BiasFieldCorrection (Tustison et al. (2010), ANTs 2.2.0), and used as T1w-reference throughout

1   the workflow. The T1w-reference was then skull-stripped using antsBrainExtraction.sh (ANTs

2   2.2.0), using OASIS as the target template. The brain mask was refined with a custom variation of

3   the method to reconcile ANTs-derived and FreeSurfer-derived segmentations of the cortical gray-

4   matter of Mindboggle (RRID:SCR_002438, Klein et al. (2017)). Spatial normalization to the ICBM

5   152 Nonlinear Asymmetrical template version 2009c (Fonov et al. (2009), RRID:SCR_008796) was

6   performed through nonlinear registration with antsRegistration (ANTs 2.2.0, RRID:SCR_004757,

7   Avants et al. (2010)), using brain-extracted versions of both T1w volume and template. Brain

8   tissue segmentation of cerebrospinal fluid (CSF), white matter (WM) and gray matter was

9   performed on the brain-extracted T1w using fast (FSL 5.0.9, RRID:SCR_002823, Zhang et al.

10 (2001)).

11 For each of the resting-state BOLD runs found per subject, the following preprocessing was

12 performed: A reference volume and its skull-stripped version were generated using a custom

13 methodology of fMRIPrep. The BOLD reference was then co-registered to the T1w reference using

14 bbregister (FreeSurfer) which implements boundary-based registration (Greve and Fischl, 2009).

15 Co-registration was configured with nine degrees of freedom to account for distortions remaining

16 in the BOLD reference. Head-motion parameters with respect to the BOLD reference

17 (transformation matrices, and six corresponding rotation and translation parameters) were

18 estimated before any spatiotemporal filtering using mcflirt (FSL 5.0.9, Jenkinson et al. (2002)).

19 BOLD runs were slice-time corrected using 3dTshift from AFNI 20160207 (Cox and Hyde (1997),

20 RRID:SCR_005927). The BOLD time-series were resampled onto MNI152NLin2009cAsym

21 standard space by applying a single, composite transform, generating a preprocessed BOLD run in

22 MNI152NLin2009cAsym space.

23 Several confounding time-series were calculated based on the preprocessed BOLD: framewise

24 displacement (FD), DVARS and three region-wise global signals (CSF, WM, and the whole-brain).

25 FD and DVARS were calculated for each functional run, both using their implementations in

26 Nipype (following the definitions by Power et al. (2014b)). The head-motion estimates calculated

27 in the correction step were also placed within the corresponding confounds file.

28 All resamplings can be performed with a single interpolation step by composing all the pertinent

29 transformations (i.e. head-motion transform matrices and co-registrations to anatomical and

1   template spaces). Gridded (volumetric) resamplings were performed using antsApplyTransforms

2   (ANTs), configured with Lanczos interpolation to minimize the smoothing effects of other kernels

3   (Lanczos, 1964).

4   Further preprocessing was performed using a confound regression procedure that has been

5   optimized to reduce the influence of participant motion (Satterthwaite et al., 2013b; Ciric et al.,

6   2017; Parkes et al., 2018); preprocessing was implemented in XCPEngine 1.0, a multi-modal

7   toolkit that deploys processing instruments from frequently used software libraries, including FSL

8   (Jenkinson et al., 2012) and AFNI (Cox, 1996). Further documentation is available at

9   https://xcpengine.readthedocs.io and https://github.com/PennBBL/xcpEngine. Functional

10 timeseries were demeaned, and linear and quadratic trends were removed. Confound regression

11 was performed using a 36-parameter model; confounds included mean signal from the whole

12 brain, WM, and CSF compartments, 6 motion parameters as well as their temporal derivatives,

13 quadratic terms, and the temporal derivatives of the quadratic terms (Satterthwaite et al., 2013a).

14 Motion censoring was applied, with outlier volumes exceeding FD = 0.5 mm or standardized

15 DVARS = 1.75 flagged and removed from confound regression. Outlier volumes were interpolated

16 over using least squares spectral analysis (Power et al., 2014a) prior to band-pass filtering to

17 retain frequencies between 0.01 Hz and 0.08 Hz, then re-censored. Prior to confound regression,

18 all confound parameters were band-pass filtered in a fashion identical to that applied to the

19 original timeseries data, ensuring comparability of the signals in frequency content (Hallquist et

20 al., 2013).

21 ***Image quality and exclusion criteria***

22 The quality of imaging data was assessed using fMRIPrep's visual reports and MRIQC 0.14.2

23 (Esteban et al., 2017). Two raters manually examined all structural and functional images

24 between preprocessing steps for image quality issues. Functional images were visually inspected

25 for whole-brain field of view coverage, signal blurring or artifacts, and proper alignment to the

26 anatomical image. Participants were excluded for: unusable anatomical image (n = 1), artifact in

27 functional data (due to hair glitter, $n = 1$), incorrect registration at the scanner ($n = 1$), average

28 FD greater than 1 mm ($n = 14$), more than 30% of resting-state frames exceeding FD > 0.5 mm

29 ($n = 8$, Power et al. (2012)). All participants that were flagged for dropout or signal blurring were

1   ultimately excluded for not meeting motion criteria. For participants with more than one usable

2   resting-state run, FD was averaged across runs, weighted by run length. All analyses controlled for

3   average FD and total number of resting-state frames.

4   To ensure that our results were not driven by motion, we conducted an additional analysis with a

5   more stringent preprocessing pipeline and motion exclusion criteria. In this pipeline, motion

6   censoring was applied with a threshold for outlier volumes of FD > 0.25 mm or standardized

7   DVARS > 1.75. One participant was lost during preprocessing as they did not have adequate

8   degrees of freedom. Additionally, we excluded participants who had average FD greater than 0.5

9   mm ($n = 8$ additional participants), for a total of $n = 83$ total participants.

10   ***Functional network analysis***

11   After preprocessing and nuisance regression, we extracted residual mean BOLD time series from a

12   400-region cortical parcellation (Schaefer et al., 2018), and represented the functional

13   connectivity matrix as a graph or network (Bassett et al., 2018). To evaluate whether our results

14   were dependent on specific node definitions, we also extracted residual mean BOLD time series

15   from a 200-region cortical parcellation (Schaefer et al., 2018). Results were qualitatively similar

16   between the two parcellations (see online at

17   https://github.com/utooley/Tooley_2022_childhood_functional_network_dev).

18   We assigned regions, or nodes, to systems based on a 7-system partition (Yeo et al., 2011), or

19   assignment of nodes to systems. Here, we use the term *system* to refer to a set of regions

20   previously defined *a priori* (i.e. the dorsal attention system, comprising a set of regions), while we

21   use the term *network* to refer to the representation of the functional connectivity matrix as a

22   graph. Regions were represented by network nodes, and the functional connectivity between

23   region i and region j was represented by the network edge between node i and node j. We used

24   this encoding of the data as a network to produce an undirected, signed, and weighted adjacency

25   matrix A. We estimated the functional connectivity between any two brain regions by calculating

26   the product-moment correlation coefficient r between the mean activity time series of region i

27   and the mean activity time series of region j (Zalesky et al., 2012). Correlations were subsequently

28   r-to-z-transformed.

1 Recent evidence has demonstrated that the maintenance of edge weights is critical for an accurate

2 understanding of the underlying biology of neural systems (Cole et al., 2012; Bassett and

3 Bullmore, 2017), and work in applied mathematics has demonstrated that graph-related

4 calculations are markedly more robust in weighted graphs than in binary graphs (Good et al.,

5 2010). In light of these two lines of evidence and recent work in the field developing methods

6 sensitive to the topologies present in weak versus strong edges (Rubinov and Sporns, 2011), we

7 maintained all edge weights without thresholding and studied the full graph including both

8 positive and negative correlations (Bassett et al., 2012; Santarnecchi et al., 2014). Functional

9 connectivity matrices were averaged across runs for each participant, weighted by the number of

10 frames in each run passing the quality threshold.

11 Across the cortex, we calculated the following summary functional network measures. *System*

12 *segregation* is a measure of segregation that quantifies the difference between mean within-

13 system connectivity and mean between-system connectivity as a proportion of mean within-

14 system connectivity (Chan et al., 2014; Wig, 2017), given an *a priori* partition of nodes into

15 systems, in this case the 7-system partition referenced earlier (Yeo et al., 2011). *Modularity*,

16 quantified by the modularity quality index (Q), is a measure of mesoscale network segregation

17 that estimates the extent to which a network's nodes can be subdivided into groups or "modules"

18 characterized by strong, dense intramodular connectivity and weak, sparse intermodular

19 connectivity. Our approach is built on the modularity quality function originally defined in

20 Newman (2006). Unlike system segregation, the modularity quality index is independent of a

21 mapping of nodes to functional systems. Higher modularity is indicative of a more highly

22 segregated network at the mesoscale. The *clustering coefficient* is a measure of local segregation

23 that quantifies the amount of connectivity between a node and its strongest neighbors (Achard et

24 al., 2006; Bartolomei et al., 2006; Bassett et al., 2006; Xu et al., 2016a). A node has a high clustering

25 coefficient when a high proportion of its neighbors are also strong neighbors of each other. The

26 *participation coefficient* quantifies the diversity of a node's connections across systems (Guimer'a

27 and Nunes Amaral, 2005; Rubinov and Sporns, 2010). A node has a high participation coefficient

28 when it is evenly and strongly connected to many different systems. A lower participation

29 coefficient is indicative of a more highly segregated network. We specifically chose measures of

30 functional network topology that were suitable for weighted, signed networks, when possible.

13

1 *System segregation*

2 System segregation quantifies the difference in mean within-system connectivity and mean

3 between-system connectivity as a proportion of within-system connectivity. Previous work has

4 linked this measure to aging-related changes in brain networks and poorer cognitive ability across

5 age (Chan et al., 2014). In these analyses, we define system segregation as in (Chan et al., 2014),

6 as:

7
$$\frac{\bar{a}_{within} - \bar{a}_{between}}{\bar{a}_{within}}$$

8 Where $\bar{a}_{within}$ is the mean edge weight between nodes within the same system and $\bar{a}_{between}$ is the

9 mean edge weight between nodes of one system to all nodes in other systems. We assigned nodes

10 to systems based on a 7-system partition (Yeo et al., 2011). Freely available MATLAB code from

11 https://github.com/mychan24/system_matrix_tools was used to calculate system segregation.

12 *Modularity quality index*

13 Statistics that quantify the modular structure of a network assess the extent to which a network's

14 nodes can be subdivided into groups or modules characterized by strong, dense intramodular

15 connectivity and weak, sparse intermodular connectivity. We considered the most commonly

16 studied mesoscale organization—assortative community structure—that is commonly assessed

17 by maximizing a modularity quality function (Porter et al., 2009; Fortunato, 2010). Our approach

18 is built on the modularity quality function originally defined by Newman (Newman, 2006) and

19 subsequently extended to weighted and signed networks by various groups.

20 Specifically, we follow Rubinov and Sporns (2011) by first letting the weight of a positive

21 connection between nodes i and j be given by a_{ij}^+ , the weight of a negative connection between

22 nodes i and j be given by $a^-{}_{ij}$, and the strength of a node i, $s_i^{\pm} = \sum_j a^{\pm}_{ij}$, be given by the sum of the

23 positive or negative j connection weights of i. We denote the chance expected within-module

24 connection weights as e_{ij}^+ for positive weights and e_{ij}^- for negative weights, where $e_{ij}^{\pm} = \frac{s_i^{\pm} s_j^{\pm}}{v^{\pm}}$. We

25 let the total weight $v^{\pm} = \sum_{ij} a_{ij}^{\pm}$ be the sum of all positive or negative connection weights in the

26 network. Then the asymmetric generalization of the modularity quality index is given by:

14

$$Q^* = \frac{1}{v^+} \sum_{ij} \left(a_{ij}^+ - e_{ij}^+\right) \delta_{M_i M_j} - \frac{1}{v^+ + v^-} \sum_{ij} \left(a_{ij}^- - e_{ij}^-\right) \delta_{M_i M_j}$$

where M_i is the community to which node i is assigned, and M_j is the community to which node j is assigned. We use a Louvain-like locally greedy algorithm as a heuristic to maximize this modularity quality index subject to a partition M of nodes into communities. We ran the Louvain algorithm 100 times per network, and detected on average 3 (M=3.44, SD =0.483) communities using modularity maximization in our developmental sample.

Clustering coefficient

To assess local network segregation, we used a commonly studied graph measure of local connectivity—the clustering coefficient— that is commonly interpreted as reflecting the capacity of the system for processing within the immediate neighborhood of a given network node (Achard et al., 2006; Bartolomei et al., 2006; Bassett and Bullmore, 2006; Xu et al., 2016b). We specifically used a formulation that was recently generalized to signed weighted networks (Zhang and Horvath, 2005; Costantini and Perugini, 2014). This version is sensitive to nonredundancy in path information based on edge sign as well as edge weight and importantly distinguishes between positive triangles and negative triangles, which have distinct meanings in networks constructed from correlation matrices.

Let the functional connectivity network of a single participant be represented as the graph $G = (V, E)$, where V and E are the vertex and edge sets, respectively. Let a_{ij} be the weight associated with the edge $(i, j) \in V$, and define the weighted adjacency matrix of G as $A = \left[a_{ij}\right]$. The clustering coefficient of node i with neighbors j and q is given by

$$C_i = \frac{\sum_{jq} \left(a_{ji} a_{iq} a_{jq}\right)}{\sum_{j \neq q} \left|a_{ji} a_{iq}\right|}$$

The clustering coefficient of the entire network was calculated as the average of the clustering coefficient across all nodes as follows:

$$C = \frac{1}{n} \sum_{i \in N} C_i$$

15

In this way, we obtained estimates of the regional and global clustering coefficient for each subject in the sample.

Participation coefficient

The participation coefficient is a measure of network integration that quantifies the diversity of a node's connections across communities, and has been linked in older children and adolescents to developmental changes in network segregation (Marek et al., 2015; Baum et al., 2017). In these analyses, we define the participation coefficient P_i of a node i as:

$$P_i = 1 - \sum_{k \in K} \left(\frac{a_{ik}}{s_i} \right)$$

where k is a system in a set K of systems, in this case defined by the a priori mapping of nodes to intrinsic functional systems (Yeo et al., 2011), a_{ik} is the positive (negative) weight of edges between node i and nodes in system k, and s_i is the positive (negative) strength of node i. The participation coefficient was calculated separately on negative and positive weights (Rubinov and Sporns, 2010).

As in our analyses of local segregation, the participation coefficient of the entire network was calculated as the average positive (negative) participation coefficient across all nodes as follows:

$$P = \frac{1}{n} \sum_{i \in N} P_i$$

The average positive and negative participation coefficient for each participant's network were averaged to obtain a global measure of network integration.

System connectivity

Within- and between-system connectivity were estimated as the average connectivity between nodes within a functional system or between pairs of functional systems. Results were corrected for multiple comparisons using the Benjamini-Hochberg false discovery rate (FDR).

16

Parcel-level connectivity

When examining results at the parcel resolution, we applied a similar model as that at the whole-brain and system level across all 79,800 edges in each child's functional brain network. As correction for multiple comparisons in this situation raises the risk of missing true effects, we alternatively employed a stringent significance threshold for display of edge-level data ($p <$ 0.001). Data are presented at $p < .01$ and at $p < .00001$ online at

https://github.com/utooley/Tooley_2022_childhood_functional_network_dev.

Statistical models

All statistical analyses were conducted in MATLAB R2018a and R 3.6.1 [@MATLAB:2018a; R Core Team (2013)]; code is publicly available at

https://github.com/utooley/Tooley_2022_childhood_functional_network_dev. We examined effects of age using generalized additive models with the *mgcv* package in R (Wood, 2011; Satterthwaite et al., 2014). We first tested for nonlinear effects of age. The penalty parameters for the nonlinear spline terms were fit as random effects and tested using restricted likelihood ratio tests (RLRTs) with *RLRsim* (Scheipl et al., 2008). Note that these tests of nonlinearity are constructed so as to test for nonlinear effects over and above any linear effects that may be present. We did not observe significant nonlinear relationships between age and whole-brain or system-level measures of network structure. 7.9% of edges showed significant nonlinear effects of age, as compared to 12.5% of edges that showed linear effects. Nonlinear effects at the parcel level are presented online at

https://github.com/utooley/Tooley_2022_childhood_functional_network_dev.

We modeled the linear effect of age while controlling for in-scanner motion (average FD), sex (male or female), total number of volumes across runs, and average functional network weight. Average network weight was included to control for global differences in connectivity strength (Van Wijk et al., 2010; Ginestet et al., 2011; Yan et al., 2013). Multiple comparisons correction was applied across models at the parcel and system resolutions using Benjamini-Hochberg false discovery rate (FDR) correction (Benjamini and Hochberg, 1995). Surfaces and partitions were shown on cortical surfaces generated by Freesurfer (Dale et al., 1999), using *fsbrain* 0.4.2 and *freesurfer-formats* 0.1.14 (Schäfer and Ecker, 2020).

Measurement and analyses of visuospatial reasoning ability

To assess reasoning, we administered matrix reasoning tests from Wechsler batteries. We used age-appropriate versions to avoid ceiling and floor effects. Children between the ages of 4 and 7 years, 7 months completed the Matrix Reasoning subtest of the Wechsler Preschool & Primary Scale of Intelligence (WPPSI-IV, Wechsler and Corporation (2012); $n = 63$). Children over age 7 years, 7 months took the Matrix Reasoning subtest of the Wechsler Intelligence Scale for Children (WISC, Wechsler et al. (2014); $n = 23$). Test items in both versions require identifying and integrating patterns in abstract shapes. For example, in Figure 4a, the foreground and background shapes switch across columns, and the shape type and color change across rows. To answer the question correctly, it is necessary to integrate these two relations. The WPPSI is normed down to 2.5 years old so it begins with simpler items than the WISC. Therefore, raw scores on the WPPSI cannot be combined with raw scores on the WISC. Age was positively associated with raw scores on the WPPSI (mean raw score: 15.31, range 3-23, max possible score: 26, $t(62) = 2.78, p = .007$). Age was not associated with raw scores on the WISC (mean raw score: 16.13, range 7-24, max possible score: 32, $t(21) = 0.40, p = .694$). Scaled scores were used for all brain analyses. Models examining relationships between reasoning and system connectivity controlled for age, sex, in-scanner motion, total number of volumes across runs, and average functional network weight. Associations between system connectivity and reasoning ability were examined only for systems showing significant associations with age and the frontoparietal system (FDR-corrected for multiple comparisons across 5 systems).

Results

Functional network segregation increases with age

We first investigated age effects on measures of whole-brain functional network segregation (Fig. 1). Measures of functional network segregation were consistently positively associated with age, including average within-system connectivity ($\beta = 0.3, t(86) = 3.75, p < .001, p_{FDR} = 0.0006$), average between-system connectivity ($\beta = -0.06, t(86) = -3.75, p < .001, p_{FDR} = 0.0006$), overall system segregation ($\beta = 0.11, t(86) = 3.60, p = .001, p_{FDR} = 0.0008$), the modularity quality index ($\beta = 0.19, t(86) = 3.06, p = .003, p_{FDR} = 0.004$), and the clustering coefficient ($\beta = 0.19, t(86) = 2.35, p = .021, p_{FDR} = 0.021$). Consistent with these associations, we found that the

18

1   average participation coefficient, a measure that inversely tracks network segregation, was

2   negatively correlated with age (β = -0.35, $t(86) = -4.68, p < .001, p_{FDR} = 0.00006$).


3
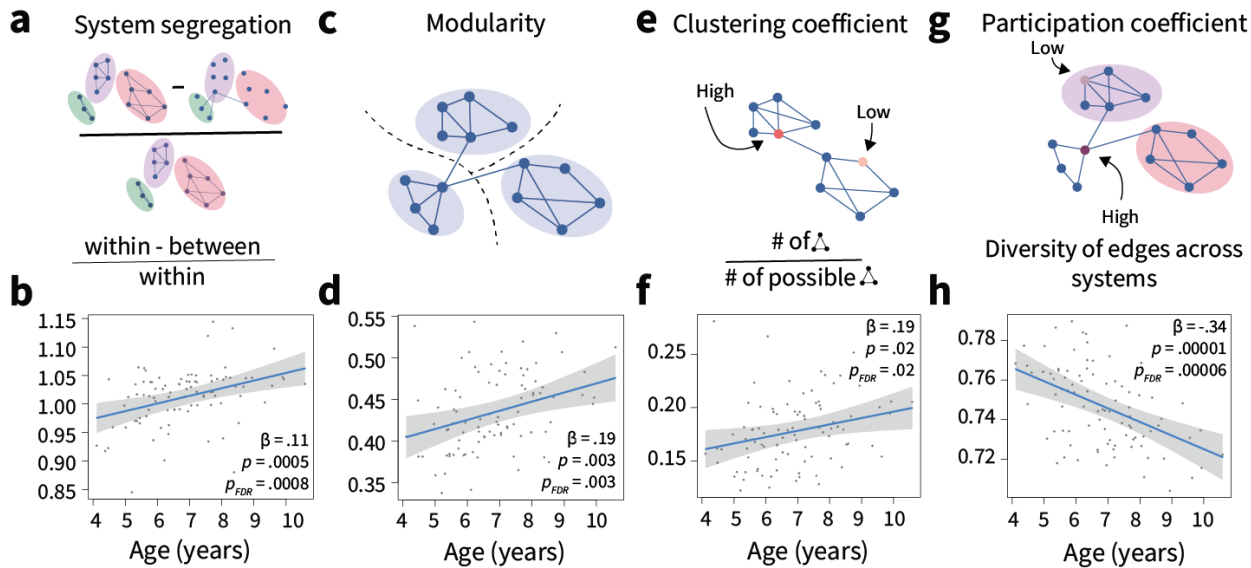
Figure 1. Functional network segregation is positively associated with age. a. System segregation is a whole-brain measure of functional network segregation that quantifies the difference between mean within-system connectivity and mean between-system connectivity as a proportion of mean within-system connectivity. **b.** System segregation is positively associated with age. **c.** Modularity is a measure of mesoscale network segregation that estimates the extent to which a network's nodes, or in this case brain regions, can be subdivided into modules characterized by strong, dense intramodular connectivity and weak, sparse intermodular connectivity. Note that the modules are data-driven, not a priori defined as functional systems. **d.** Modularity is positively associated with age. **e.** The clustering coefficient is a measure of local segregation that quantifies the amount of connectivity between a node and its neighbors. A node has a high clustering coefficient when a high proportion of its neighbors are also strongly connected to one another. In a weighted network, the clustering coefficient measures the strength of triangles around a node. **f.** The average clustering coefficient is positively associated with age. **g.** The participation coefficient quantifies the diversity of a node's connections across systems. A node has a high participation coefficient when it is evenly connected to many different systems. A lower participation coefficient is indicative of a more segregated network. **h.** The average participation coefficient is negatively associated with age.

Systems specializing in perceptual processing segregate from systems for abstract thought

19   We next tested for age effects at the system level by dividing the cortex into seven systems (Yeo et

20   al., 2011). We first visualized the balance of significant positive and negative age effects within and

21   between systems (Fig. 2a). Within systems, 94.6% of significant age effects were positive and 5.3%

22   were negative. Between systems, 27.7% of significant age effects were positive and 72.2% were

19

1 negative. Age was positively, but weakly, associated with within-system connectivity in the visual

2 (Fig. 2b, $\beta = 0.25, t(86) = 2.51, p = .014$) and default mode systems ($\beta = 0.24, t(86) = 2.42, p =$

3 $.017$), as well as in the ventral attention system ($\beta = 0.24, t(86) = 2.41, p = .018$). The

4 significance of these associations did not survive correction for multiple comparisons. In contrast,

5 age was strongly associated with between-system connectivity (Fig. 2c). Age was negatively

6 associated with connectivity between the default mode and dorsal attention systems ($\beta = -0.24,$

7 $t(86) = -3.79, p < .001, p_{FDR} = 0.01$), and connectivity between the default mode and ventral

8 attention systems ($\beta = -0.22, t(86) = -3.36, p = .001, p_{FDR} = 0.02$). Additionally, age was

9 positively correlated with connectivity between the visual and dorsal attention systems ($\beta = 0.32,$

10 $t(86) = 3.15, p = .002, p_{FDR} = 0.02$) and with connectivity between the dorsal attention and

11 ventral attention systems ($\beta = 0.22, t(86) = 2.92, p = .004, p_{FDR} = 0.03$).
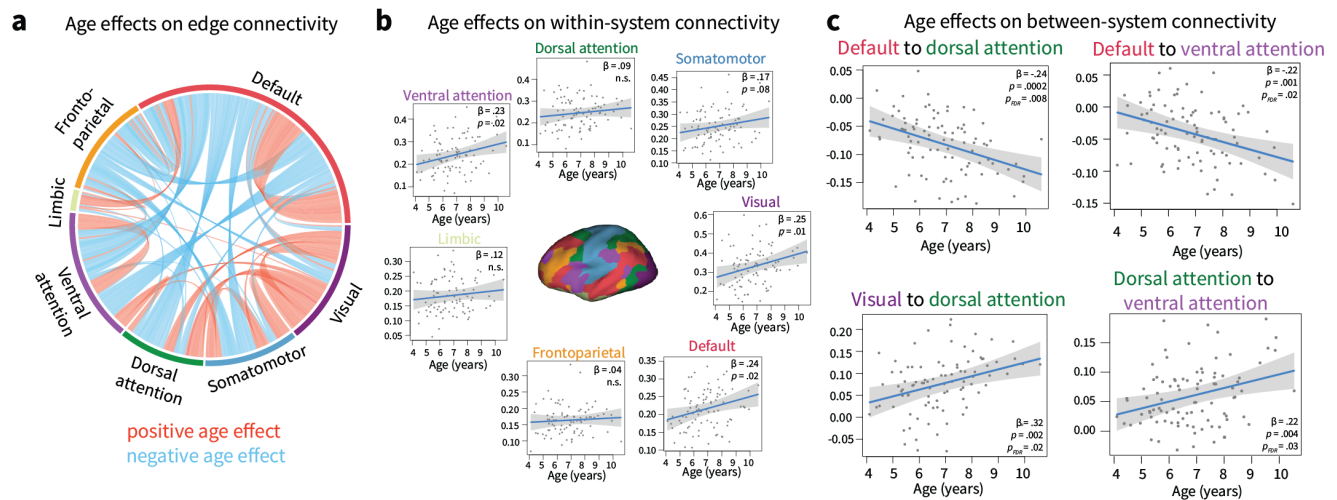

13 **Figure 2. System-level effects of age on system connectivity. a.** Age effects on edge connectivity. Note that only

14 edges with significant age effects at $p_{unc} < 0.001$ are shown. **b.** Age effects on within-system connectivity. No

15 relationships survive FDR correction across systems. **c.** Age effects on between-system connectivity. All effects shown

16 survive FDR correction across systems.

17 *Age effects are concentrated at both ends of the sensory-association gradient*

18 We next examined age effects at the parcel level to characterize regional specificity. In particular,

19 we determined which parcels had the most edges with significant age effects. Parcels with the

20 highest number of positive edge-level age effects were observed in the intraparietal sulcus (2

21 parcels with 9 significant edges), the medial prefrontal cortex (7 edges), and the occipital cortex (6

1 edges; see Fig. 3a). When parcels were grouped by system (Yeo et al., 2011), positive associations

2 with age were most common in the visual system, followed by the default mode system, and the

3 ventral attention system (Fig. 3b). Parcels with negative edge-level age effects were also

4 concentrated in the medial prefrontal cortex and the intraparietal sulcus, but not in lower-level

5 sensory or motor areas (Fig. 3c). Edge-level age effects were most pronounced in a medial

6 prefrontal cortex parcel in the default mode system (top parcel: medial prefrontal cortex, 13

7 negative age-associated edges). The top five non-anatomical meta-analytic associations on

8 Neurosynth for the medial prefrontal cortex region (MNI coordinates of centroid: x = 8, y = 54, z =

9 12) were "mind," "theory mind," "autobiographical," "mentalizing," and "mental states". Negative

10 associations with age were most common in the default mode system and the ventral attention

11 system, followed by the dorsal attention and frontoparietal systems. Very few negative

12 associations were found in the visual, somatomotor, or limbic systems (Fig. 3d).
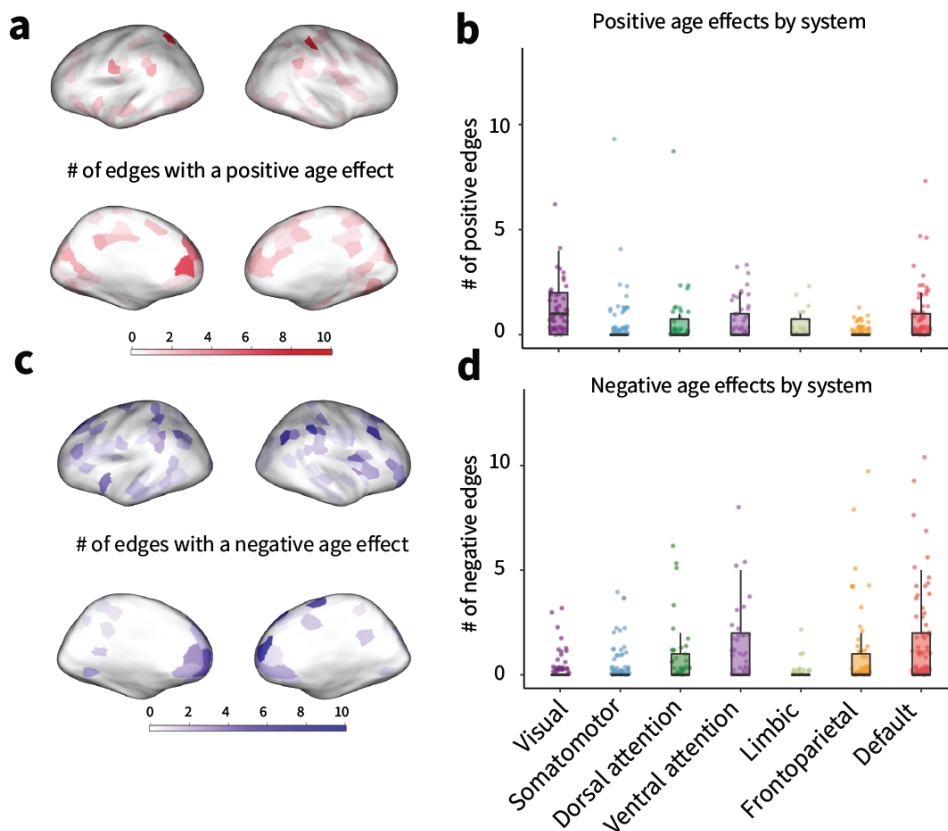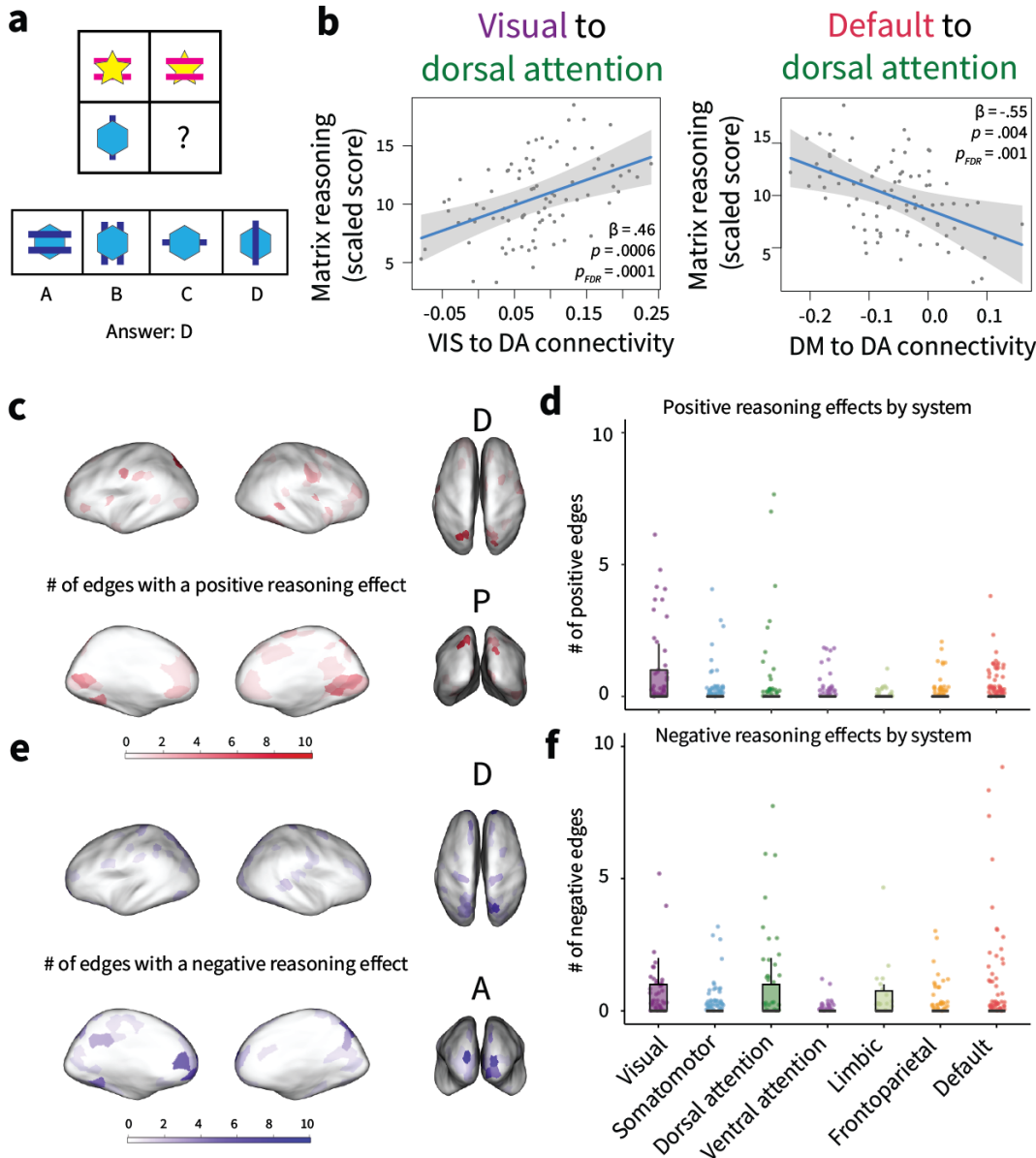

13

14 **Figure 3. Parcel-level effects of age on network connectivity. a.** Number of edges from each parcel showing a

15 significant positive age association; significance was defined as $p_{unc} < 0.001$. **b.** Number of edges with positive effects

16 of age, grouped by system. Each datapoint represents a parcel. **c.** Number of edges from each parcel showing a

1   significant negative age association; significance was defined as $p_{unc} < 0.001$. **d.** Negative edge effects for each parcel

2   grouped by system. Each datapoint represents a parcel.

Functional network structure is associated with cognition

4   Finally, we explored the cognitive consequences of age-associated network segregation by

5   examining relationships between functional architecture and visuospatial reasoning (matrix

6   reasoning from Wechsler tests (Wechsler and Corporation, 2012; Wechsler et al., 2014); see Fig.

7   4a). Controlling for age, reasoning was positively associated with average within-system

8   connectivity ($\beta = 0.34$, $F(1,79) = 4.78$, $p = .032$, $p_{FDR} = 0.08$), and negatively associated with

9   average between-system connectivity ($\beta = $ -1.57, $F(1,79) = 4.78$, $p = .032$, $p_{FDR} = 0.08$) and

10 average participation coefficient ($\beta = $ -0.35, $F(1,79) = 4.39$, $p = .039$, $p_{FDR} = 0.08$). However,

11 these associations did not pass correction for multiple comparisons, and reasoning was not

12 associated with other measures of whole-brain network architecture (p-values > .05). At the

13 system level, we focused on pairs of cognitive systems that show significant associations with age

14 (see Fig. 2c), and found that connectivity between the visual and dorsal attention systems was

15 positively associated with reasoning ability (Fig. 4b, $\beta = 0.46$, $t(79) = 4.06$, $p < .001$, $p_{FDR} = $

16 0.0006). We also found that connectivity between the default and dorsal attention systems was

17 negatively associated with reasoning ability (Fig. 4b, $\beta = $ -0.55, $t(79) = -2.93$, $p = .004$, $p_{FDR} = $

18 0.01). Further, motivated by prior studies linking the frontoparietal system to reasoning (Prado et

19 al., 2011; Wertheim and Ragni, 2018), we tested whether reasoning was associated with within-

20 system frontoparietal connectivity; we found no effect ($\beta = 0.07$, $t(79) = 0.51$, $p = .613$, $p_{FDR} = $

21 0.68). At the parcel level, connections with the intraparietal sulcus (top parcel: 8 edges), as well as

22 the medial prefrontal and occipital areas, showed positive relationships with reasoning (Fig. 4c).

23 Parcels with positive reasoning effects were most numerous in the visual system (Fig. 4d).

24 Connections with the frontal pole (top parcel: 8 edges), the intraparietal sulcus, the medial

25 prefrontal cortex, and visual areas showed negative associations with reasoning (Fig. 4e). Parcels

26 with negative reasoning effects were most numerous in the visual, default mode, and dorsal

27 attention systems (Fig. 4f).

Figure 4. Associations between functional network structure and visuospatial reasoning. a. Example reasoning item. Reasoning was assessed with the Matrix Reasoning subscale of the Weschler assessments. **b.** System-level associations with reasoning, controlling for age. Reasoning is associated with connectivity between the visual and dorsal attention systems, and with connectivity between the default mode and dorsal attention systems. **c.** The number of edges from each parcel showing a significant positive reasoning association; significance was defined as $p_{unc} < 0.001$. **d.** The number of edges with positive effects of reasoning, grouped by system. Each datapoint represents a parcel. **e.** The number of edges from each parcel showing a significant negative reasoning association; significance was defined as $p_{unc} < 0.001$. **f.** The number of edges with negative effects of reasoning, grouped by system. Each datapoint represents a parcel.

23

1   *Sensitivity analyses*

2   We conducted a set of sensitivity analyses to ensure that our results were not dependent on

3   specific analytical choices. Specifically, we conducted our main analyses with a more stringent

4   preprocessing pipeline and motion exclusion criteria. In this pipeline, measures of functional

5   network segregation were consistently positively associated with age, including average within-

6   system connectivity ($\beta = 0.22, t(77) = 3.02, p = .003, p_{FDR} = 0.007$), average between-system

7   connectivity ($\beta = $ -0.04, $t(77) = -3.02, p = .003, p_{FDR} = 0.007$), overall system segregation ($\beta = $

8   $0.1, t(77) = 2.53, p = .013, p_{FDR} = 0.01$), the modularity quality index ($\beta = 0.23, t(77) = 3.74,$

9   $p < .001, p_{FDR} = 0.002$), and the clustering coefficient ($\beta = 0.21, t(77) = 2.67, p = .009, p_{FDR} = $

10 0.01). Consistent with these associations, we found that the average participation coefficient, a

11 measure that inversely tracks network segregation, was negatively correlated with age ($\beta = $ -0.23,

12 $t(77) = -2.66, p = .009, p_{FDR} = 0.01$, see Fig. 5a).

13 At the system resolution, age was positively, but weakly, associated with within-system

14 connectivity in the visual ($\beta = 0.25, t(77) = 2.21, p = .030$) and limbic ($\beta = 0.2, t(77) = 2.05, p = $

15 $.044$) systems, and was marginally positively associated with within-system connectivity in the

16 default mode ($\beta = 0.17, t(77) = 1.83, p = .071$) and somatomotor systems ($\beta = 0.18, t(77) = $

17 $1.93, p = .057$). None of these associations survived correction for multiple comparisons. In

18 contrast, age was strongly associated with between-system connectivity (Fig. 5b). Age was

19 negatively associated with connectivity between the default mode and ventral attention system

20 ($\beta = $ -0.17, $t(77) = -3.09, p = .003, p_{FDR} = 0.04$). Age was also negatively associated with

21 connectivity between the default mode and dorsal attention system ($\beta = $ -0.17, $t(77) = -2.66,$

22 $p = .009, p_{FDR} = 0.09$), but this association was marginal after FDR correction. Additionally, age

23 was positively correlated with connectivity between the visual and dorsal attention systems ($\beta = $

24 $0.36, t(77) = 3.64, p < .001, p_{FDR} = 0.01$).

25 We next examined age effects at the parcel level to characterize regional specificity. Parcels with

26 the highest number of positive edge-level age effects were observed in the superior parietal

27 lobule/intraparietal sulcus (2 parcels with 11 and 9 significant edges) and the occipital cortex (2

28 parcels with 10 and 9 significant edges; see Fig. 5d). Parcels with the highest number of negative

1   edge-level age effects occurred in medial prefrontal cortex (8 edges) and intraparietal sulcus (7

2   edges, Fig. 5e).

3   Finally, we examined relationships between functional architecture and visuospatial reasoning.

4   Controlling for age, reasoning was marginally positively associated with average within-system

5   connectivity ($\beta = 0.32$, $F(1,72) = 2.96$, $p = .090$, $p_{FDR} = 0.18$), and marginally negatively

6   associated with average between-system connectivity ($\beta = $ -1.62, $F(1,72) = 2.96$, $p = .090$,

7   $p_{FDR} = 0.18$). However, these associations did not pass correction for multiple comparisons, and

8   reasoning was not associated with other measures of whole-brain network architecture (p-values

9   > .05). At the system level, we focused on pairs of cognitive systems that showed associations with

10 age in the main analyses, and found that connectivity between the visual and dorsal attention

11 systems was positively associated with reasoning ability (Fig. 5e, $\beta = 0.51$, $t(72) = 4.00$, $p < .001$,

12 $p_{FDR} = 0.0008$). We also found that connectivity between the default and dorsal attention systems

13 was negatively associated with reasoning ability ($\beta = $ -0.72, $t(72) = -3.51$, $p = .001$, $p_{FDR} = $

14 0.0019). Reasoning was not associated with within-system frontoparietal connectivity ($\beta = 0.17$,

15 $t(72) = 1.01$, $p = .318$, $p_{FDR} = 0.53$). At the parcel level, connections with superior parietal cortex

16 (8 edges) and visual areas (7 edges) showed positive relationships with reasoning (Fig. 5f).

17 Connections with the frontal pole (7 edges), superior parietal cortex (2 parcels with 7 and 6

18 edges), medial prefrontal cortex (6 edges), and visual areas showed negative associations with

19 reasoning (Fig. 5g).
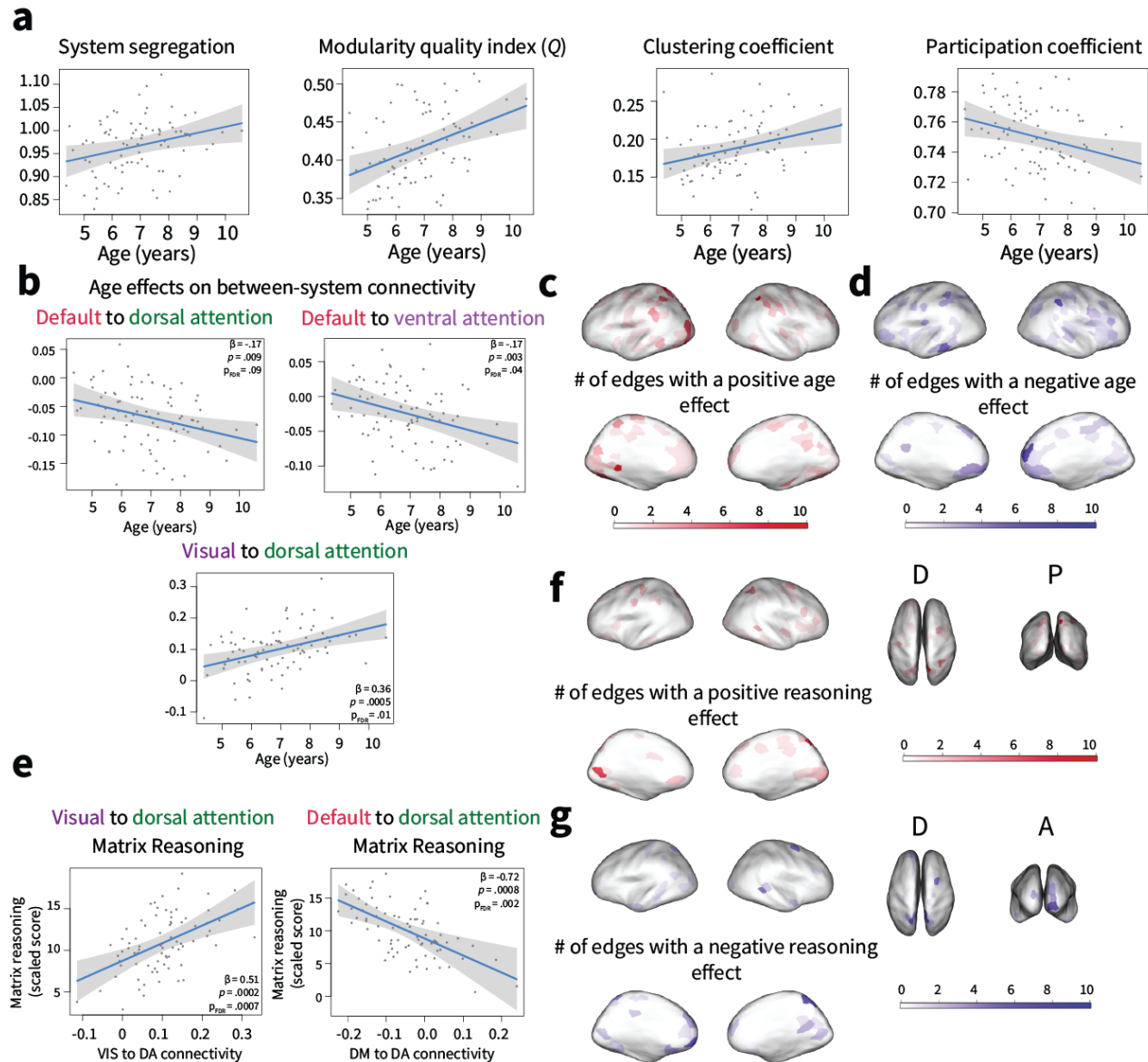
Figure 5. Replication with stricter motion exclusions. In this pipeline, we censored volumes with FD > 0.25mm and excluded participants with average FD > 0.5 mm. **a.** Whole-brain measures of functional network segregation (system segregation, modularity, and the clustering coefficient) are positively associated with age. The participation coefficient is a measure of functional network integration and is negatively associated with age. **b.** Age effects on between-system connectivity. **c.** Number of edges from each parcel showing a significant positive age association; significance was defined as $p_{unc} < 0.001$. **d.** Number of edges from each parcel showing a significant negative age association; significance was defined as $p_{unc} < 0.001$. **e.** System-level associations with reasoning, controlling for age. Reasoning is associated with connectivity between the visual and dorsal attention systems, and with connectivity between the default mode and dorsal attention systems. **f.** The number of edges from each parcel showing a

26

1 significant positive reasoning association; significance was defined as $p_{unc} < 0.001$. **g.** The number of edges from each

2 parcel showing a significant negative reasoning association; significance was defined as $p_{unc} < 0.001$.

Discussion

4 We investigated the development of cortical functional network architecture during childhood. At

5 the whole-brain level, age was positively associated with multiple measures of functional network

6 segregation, consistent with prior work on development later in childhood and adolescence (Fair

7 et al., 2009; Marek et al., 2015; Lopez et al., 2019). At the system level, age was associated with a

8 segregation of systems involved in attention from those involved in abstract, internally oriented

9 cognition, as well as an integration among attentional and perceptual systems. At the parcel level,

10 age effects on functional connectivity were strongest in medial prefrontal areas of the default

11 mode system, and in areas of the visual system. Classically, brain development is thought to move

12 from back to front, from sensory areas to association areas. Our results suggest another

13 possibility: both ends of the sensory-association gradient are anchored early, perhaps by the

14 presence or absence of sensory input, and then boundaries along the gradient are gradually

15 solidified. This possibility is consistent with the very early emergence of the default mode network

16 in utero and in infancy (Gao et al., 2009; Thomason et al., 2014; Gilmore et al., 2018; Hodel, 2018),

17 and with work showing that medial prefrontal cortex, like primary sensory areas, is already highly

18 segregated in adolescence (Baum et al., 2020). These findings fill a critical gap in our

19 understanding of how intrinsic functional network remodeling supports the profound cognitive

20 development that takes place during early and middle childhood.

21 Age effects were pronounced in areas of medial prefrontal cortex that are activated by self-

22 referential thought and social perception tasks in adults (de la Vega et al., 2016; Meyer and

23 Lieberman, 2018; Parelman et al., 2021). This result is consistent with evidence for major changes

24 in social cognition between the ages of 3 and 10 years, supported by changes in the structure and

25 function of the medial prefrontal cortex, the precuneus, and the temporoparietal junction (Weimer

26 et al., 2021). Though we did not collect a behavioral or imaging measure of social cognition in this

27 sample, we speculate that the medial prefrontal regions that show age effects may support

28 improvements in social cognition in this age range. In this context, it is notable that medial

29 prefrontal cortex continues developing after 10 years of age, and shows a protracted course of

1   age-associated change through adolescence and into adulthood (Baum et al., 2020). The age-

2   associated remodeling we observe in medial prefrontal cortex may be simply an early

3   manifestation of the ongoing anchoring of the far end of the sensorimotor-association gradient

4   that continues into adulthood. It is also possible that changes in medial prefrontal connectivity

5   more broadly support self-regulation processes that are required for efficiently completing most

6   types of tasks (Akshoomoff et al., 2014; de la Vega et al., 2016; Meyer and Lieberman, 2018).

7   Age effects were also pronounced in the visual system. The visual network showed increased

8   integration with the dorsal attention network, particularly along the dorsal stream. The majority

9   of inputs into primary visual cortex come from higher-order visual areas and attention areas

10   (Muckli and Petro, 2013), so it is possible that inputs from attention systems are reflected in the

11   structure and function of perceptual areas. Indeed, attention improves substantially in early

12   childhood (Amso and Scerif, 2015). Further, connectivity within regions of the dorsal attention

13   and visual systems is positively associated with attention skills in 4-7-year-old children (Rohr et

14   al., 2017, 2018), suggesting that the age effects we observe in regions of the visual system may

15   also support developing attention skills.

16   Better reasoning abilities were associated with more mature patterns of brain network

17   architecture, after controlling for age. At the parcel level, reasoning was associated with the

18   connectivity of medial prefrontal and visual areas, as well as the intraparietal sulcus and the

19   frontal pole. At the systems level, reasoning was associated with integration between the visual

20   and dorsal attention systems, and with segregation between the default mode and dorsal attention

21   systems. Prior work in older children and adults has linked structure and function of the

22   frontoparietal system to reasoning skills, with a specific focus on rostral lateral prefrontal cortex

23   and parietal areas (Prado et al., 2011; Vendetti and Bunge, 2014; Wertheim and Ragni, 2018).

24   Interestingly, one study found that neural correlates of reasoning depended on age: after age 8

25   years, stronger reasoning skills were associated with stronger functional connectivity between

26   rostral lateral prefrontal cortices and the inferior parietal lobe, whereas before age 8 years, there

27   were no such associations (Wendelken et al., 2016). Similarly, we found no association between

28   frontoparietal system connectivity and reasoning ability in our age range. By taking a whole brain

29   approach rather than focusing on the frontoparietal network, we found that visuospatial

30   reasoning is associated with integration between perceptual and attentional systems in children.

28

1   We also found that reasoning was associated with segregation between task-positive and task-

2   negative systems, consistent with other work across multiple age ranges and cognitive domains

3   (Chan et al., 2014; Keller et al., 2015; Marek et al., 2019; Bruchhage et al., 2020). The involvement

4   of perceptual systems such as the visual and dorsal attention systems in reasoning may not be as

5   surprising as it initially seems: in children and adults, reasoning tasks engage visual areas more

6   than non-reasoning control tasks (Souli'eres et al., 2009; Mackey et al., 2015; Whitaker et al.,

7   2018). There is also evidence that reasoning performance relies more on lower-level skills like

8   processing speed and visuospatial attention than on higher-level skills like working memory and

9   relational integration early in childhood (Fry and Hale, 1996; Kail and Hulme, 2016). Broadly, our

10   results suggest that maturation of brain network architecture, in particular in areas at two ends of

11   the sensory-association gradient, supports the development of reasoning abilities.

12   Making decisions about motion criteria is difficult because of tradeoffs between data quality and

13   generalizability, as motion is often highly correlated with other sample characteristics of interest

14   (Hodgson et al., 2017; Leonard et al., 2017; Bolton et al., 2019). Our approach here was to analyze

15   the data at two motion thresholds, a more lenient threshold that included more children and more

16   data, and a more conservative threshold that minimized motion concerns. At both thresholds, the

17   general pattern of findings was the same. At the whole-brain level, age was positively associated

18   with measures of segregation. At the system level, age was positively associated with segregation

19   between external and internal attention systems, and integration between attentional and

20   perceptual systems. Although the specific parcel-level results were not identical, the broad pattern

21   of results is similar, with age effects on functional connectivity strongest in medial prefrontal

22   cortex, superior parietal cortex, and visual areas. Better reasoning abilities were associated with

23   more mature patterns of brain network architecture. This suggests that our findings are robust

24   and are not driven by motion.

25   Several potential limitations should be noted. First, our dataset is cross-sectional and of a

26   relatively small sample size. Future work with longitudinal data will be necessary to establish the

27   temporal sequence of the relationships we report, as well as to better evaluate nonlinearities and

28   ideally, developmental trajectories in children younger than age 4 years. Longitudinal data would

29   also make it possible to test whether changes in network structure mediate age-related

30   improvements in reasoning. Fortunately, such a study — the HEALthy Brain and Cognitive

1   Development Study (Volkow et al., 2020) — is about to begin. Second, by carefully excluding data

2   with motion artifacts, we may have limited the generalizability of our findings. Most young

3   children move in the scanner, so it is essential to develop more motion-resilient sequences to

4   allow investigators to acquire data in a more representative sample of young kids. Third, our

5   cognitive measures were limited. Future work is necessary to link changes in functional

6   organization to changes across a broader set of cognitive and social skills, including abilities that

7   might diminish with age, such as creativity and imagination (Thompson-Schill et al., 2009; Gopnik,

8   2020). Fourth, major cognitive and social changes during middle childhood (called the "age of

9   reason" by anthropologists Sameroff and Haith (1996)) have been observed across many cultures

10   all over the world, but our sample only captures development in our specific geographic and

11   cultural context. Finally, we could not determine the causes of the developmental patterns we

12   uncovered. More work is needed to understand whether these patterns were associated with

13   specific experiences, for example formal schooling (Brod et al., 2017; Nolden et al., 2021), or

14   simply reflect biological experience-independent maturation.

15   In sum, age effects on functional cortical architecture during childhood parallel long-known age

16   effects on behavior. As children learn to resist the lure of perceptual information, and begin to

17   reason abstractly, cortical systems for perception and abstraction separate, while connections that

18   facilitate attention tend to strengthen. As children's concept of self matures, the connectivity of the

19   medial prefrontal cortex changes. Our results provide new insights into how changes in cortical

20   organization give rise to changes in the mind as children reach the age of reason.

21   **Citation diversity statement**

22   Recent work in several fields of science—including neuroscience, where our work here is

23   situated—has identified a bias in citation practices such that papers from women and other

24   marginalized scholars are under-cited relative to the number of such papers in the field (Maliniak

25   et al., 2013; Mitchell et al., 2013; Caplar et al., 2017; Dion et al., 2018; Dworkin et al., 2020;

26   Chatterjee and Werner, 2021; Teich et al., 2021; Wang et al., 2021). Here we sought to proactively

27   consider choosing references that reflect the diversity of the field in thought, form of contribution,

28   gender, race, ethnicity, and other factors. First, we obtained the predicted gender of the first and

29   last author of each reference by using databases that store the probability of a first name being

1   carried by a woman (Dworkin et al., 2020; Zhou et al., 2020). By this measure (and excluding self-

2   citations to the first and last authors of our current paper), our references contain 26%

3   woman(first)/woman(last), 16% man/woman, 20% woman/man, and 38% man/man

4   categorization. This method is limited in that a) names, pronouns, and social media profiles used

5   to construct the databases may not, in every case, be indicative of gender identity and b) it cannot

6   account for intersex, non-binary, or transgender people. Second, we obtained the predicted

7   racial/ethnic category of the first and last author of each reference by databases that store the

8   probability of a first and last name being carried by an author of color (Ambekar et al., 2009; Sood

9   and Laohaprapanon, 2018). By this measure (and excluding self-citations), our references contain

10   9.83% author of color (first)/author of color(last), 16.45% white author/author of color, 18.51%

11   author of color/white author, and 55.21% white author/white author. This method is limited in

12   that a) names and Florida Voter Data to make the predictions may not be indicative of

13   racial/ethnic identity, and b) it cannot account for Indigenous and mixed-race authors, or those

14   who may face differential biases due to the ambiguous racialization or ethnicization of their

15   names. We look forward to future work that could help us to better understand how to support

16   equitable practices in science.

Author contributions

18   U.A. Tooley, D.S. Bassett, and A.P. Mackey developed the study concept. All authors contributed to

19   the study design. Testing and data collection were performed by U.A. Tooley, A.T. Park, J.A.

20   Leonard, A.L. Boroshok, and C.L. McDermott. U.A. Tooley performed the data analysis and

21   interpretation under the supervision of A.P. Mackey and D.S. Bassett. U.A. Tooley and A.P. Mackey

22   drafted the manuscript, and A.T. Park, J.A. Leonard, A.L. Boroshok, C.L. McDermott, and D.S. Bassett

23   provided critical revisions. All authors approved the final version of the manuscript for

24   submission.

Acknowledgements

References

Achard S, Salvador R, Whitcher B, Suckling J, Bullmore E (2006) A resilient, low-frequency, small-world human brain functional network with highly connected association cortical hubs. Journal of Neuroscience 26:63–72.

Akshoomoff N et al. (2014) The NIH Toolbox Cognition Battery: Results from a Large Normative Developmental Sample (PING). Neuropsychology 28:1–10.

Ambekar A, Ward C, Mohammed J, Male S, Skiena S (2009) Name-ethnicity classification from open sources. In: Proceedings of the 15th ACM SIGKDD international conference on knowledge discovery and data mining, pp 49–58.

Amso D, Scerif G (2015) The attentive brain: Insights from developmental cognitive neuroscience. Nature Reviews Neuroscience 16:606–619.

Avants BB, Yushkevich P, Pluta J, Minkoff D, Korczykowski M, Detre J, Gee JC (2010) The Optimal Template Effect in Hippocampus Studies of Diseased Populations. NeuroImage 49:2457.

Bartolomei F, Bosma I, Klein M, Baayen JC, Reijneveld JC, Postma TJ, Heimans JJ, van Dijk BW, de Munck JC, de Jongh A, Cover KS, Stam CJ (2006) Disturbed functional connectivity in brain tumour patients: Evaluation by graph analysis of synchronization matrices. Clinical Neurophysiology 117:2039–2049.

Bassett DS, Bullmore E (2006) Small-world brain networks. The Neuroscientist 12:512–523.

Bassett DS, Bullmore ET (2017) Small-world brain networks revisited. The Neuroscientist 23:499–516.

Bassett DS, Meyer-Lindenberg A, Achard S, Duke T, Bullmore E (2006) Adaptive reconfiguration of fractal small-world human brain functional networks. Proceedings of the National Academy of Sciences 103:19518–19523.

Bassett DS, Nelson BG, Mueller BA, Camchong J, Lim KO (2012) Altered resting state complexity in schizophrenia. Neuroimage 59:2196–2207.

Bassett DS, Zurn P, Gold JI (2018) On the nature and use of models in network neuroscience. Nature Reviews Neuroscience 19:566.

Baum GL, Ciric R, Roalf DR, Betzel RF, Moore TM, Shinohara RT, Kahn AE, Vandekar SN, Rupert PE, Quarmley M, Cook PA, Elliott MA, Ruparel K, Gur RE, Gur RC, Bassett DS, Satterthwaite TD (2017) Modular segregation of structural brain networks supports the development of executive function in youth. Current Biology 27:1561–1572.

Baum GL, Cui Z, Roalf DR, Ciric R, Betzel RF, Larsen B, Cieslak M, Cook PA, Xia CH, Moore TM, Ruparel K, Oathes DJ, Alexander-Bloch AF, Shinohara RT, Raznahan A, Gur RE, Gur RC, Bassett DS, Satterthwaite TD (2020) Development of structurefunction coupling in human brain networks during youth. Proc Natl Acad Sci USA 117:771–778.

Benjamini Y, Hochberg Y (1995) Controlling the false discovery rate: A practical and powerful approach to multiple testing. Journal of the Royal Statistical Society Series B (Methodological) 57:289–300.

Bolton TAW, Kebets V, Glerean E, Zöller D, Li J, Yeo BTT, Caballero-Gaudes C, Van De Ville D (2019) Agito ergo sum: Correlates of spatio-temporal motion characteristics during fMRI. NeuroImage:116433.

Brod G, Bunge SA, Shing YL (2017) Does One Year of Schooling Improve Children's Cognitive Control and Alter Associated Brain Activation? Psychological Science 28:967–978.

Brown TT, Jernigan TL (2012) Brain development during the preschool years. Neuropsychology Review 22:313–333.

Bruchhage MMK, Ngo G-C, Schneider N, D'Sa V, Deoni SCL (2020) Functional connectivity correlates of infant and early childhood cognitive development. Brain Structure and Function 225:669–681.

Buckner RL, DiNicola LM (2019) The brain's default network: Updated anatomy, physiology and evolving insights. Nature Reviews Neuroscience.

Caplar N, Tacchella S, Birrer S (2017) Quantitative evaluation of gender bias in astronomical publications from citation counts. Nature Astronomy 1:1–5.

Cardin JA (2018) Inhibitory Interneurons Regulate Temporal Precision and Correlations in Cortical Circuits. Trends in Neurosciences 41:689–700.

Chai XJ, Ofen N, Gabrieli JDE, Whitfield-Gabrieli S (2013) Selective Development of Anticorrelated Networks in the Intrinsic Functional Organization of the Human Brain. Journal of Cognitive Neuroscience 26:501–513.

Chan MY, Park DC, Savalia NK, Petersen SE, Wig GS (2014) Decreased segregation of brain systems across the healthy adult lifespan. Proceedings of the National Academy of Sciences 111:E4997–E5006.

Chandler M, Lalonde C (1996) Shifting to an interpretive theory of mind: 5- to 7-year-olds' changing conceptions of mental life. In: The five to seven year shift: The age of reason and responsibility, pp 111–139 The John D. And Catherine T. MacArthur Foundation series on mental heath and development. Chicago, IL, US: University of Chicago Press.

Chatterjee P, Werner RM (2021) Gender Disparity in Citations in High-Impact Journal Articles. JAMA network open 4:e2114509.

Chen J, Tam A, Kebets V, Orban C, Ooi LQR, Marek S, Dosenbach N, Eickhoff S, Bzdok D, Holmes AJ, Yeo BTT (2020) Shared and unique brain network features predict cognition, personality and mental health in childhood. bioRxiv:2020.06.24.168724.

Chini M, Pfeffer T, Hanganu-Opatz IL (2021) Developmental increase of inhibition drives decorrelation of neural activity. bioRxiv:2021.07.06.451299.

Ciric R, Rosen AFG, Erus G, Cieslak M, Adebimpe A, Cook PA, Bassett DS, Davatzikos C, Wolf DH, Satterthwaite TD (2018) Mitigating head motion artifact in functional connectivity MRI. Nature Protocols:1.

Ciric R, Wolf DH, Power JD, Roalf DR, Baum GL, Ruparel K, Shinohara RT, Elliott MA, Eickhoff SB, Davatzikos C, Gur RC, Gur RE, Bassett DS, Satterthwaite TD (2017) Benchmarking of participant-level confound regression strategies for the control of motion artifact in studies of functional connectivity. NeuroImage 154:174–187.

Cole M, Cole SR, Lightfoot C (2005) The development of children. Macmillan.

Cole MW, Reynolds JR, Power JD, Repovs G, Anticevic A, Braver TS (2013) Multi-task connectivity reveals flexible hubs for adaptive task control. Nature neuroscience 16:1348–1355.

Cole MW, Yarkoni T, Repovš G, Anticevic A, Braver TS (2012) Global Connectivity of Prefrontal Cortex Predicts Cognitive Control and Intelligence. J Neurosci 32:8988–8999.

Corbetta M, Shulman GL (2002) Control of goal-directed and stimulus-driven attention in the brain. Nature Reviews Neuroscience 3:201–215.

Costantini G, Perugini M (2014) Generalization of clustering coefficients to signed correlation networks. PLOS ONE 9:e88669.

Cox RW (1996) AFNI: Software for analysis and visualization of functional magnetic resonance neuroimages. Computers and Biomedical Research, an International Journal 29:162–173.

Cox RW, Hyde JS (1997) Software tools for analysis and visualization of fMRI data. NMR in Biomedicine 10:171–178.

Dale AM, Fischl B, Sereno MI (1999) Cortical Surface-Based Analysis: I. Segmentation and Surface Reconstruction. NeuroImage 9:179–194.

de la Vega A, Chang LJ, Banich MT, Wager TD, Yarkoni T (2016) Large-Scale Meta-Analysis of Human Medial Frontal Cortex Reveals Tripartite Functional Organization. The Journal of Neuroscience 36:6553–6562.

1 Dhamala E, Jamison KW, Jaywant A, Dennis S, Kuceyeski A (2021) Distinct functional and
2 structural connections predict crystallised and fluid cognition in healthy adults. Human Brain
3 Mapping 42:3102–3118.

4 Dion ML, Sumner JL, Mitchell SM (2018) Gendered citation patterns across political science and
5 social science methodology fields. Political Analysis 26:312–327.

6 Dong H-M, Margulies DS, Zuo X-N, Holmes AJ (2021) Shifting gradients of macroscale cortical
7 organization mark the transition from childhood to adolescence. Proceedings of the National
8 Academy of Sciences 118.

9 Dosenbach NUF, Koller JM, Earl EA, Miranda-Dominguez O, Klein RL, Van AN, Snyder AZ, Nagel BJ,
10 Nigg JT, Nguyen AL, Wesevich V, Greene DJ, Fair DA (2017) Real-time motion analytics during
11 brain MRI improve data quality and reduce costs. NeuroImage 161:80–93.

12 Dworkin JD, Linn KA, Teich EG, Zurn P, Shinohara RT, Bassett DS (2020) The extent and drivers of
13 gender imbalance in neuroscience reference lists. Nature Neuroscience 23:918–926.

14 Esteban O, Birman D, Schaer M, Koyejo OO, Poldrack RA, Gorgolewski KJ (2017) MRIQC:
15 Advancing the automatic prediction of image quality in MRI from unseen sites. PLOS ONE
16 12:e0184661.

17 Esteban O, Markiewicz CJ, Blair RW, Moodie CA, Isik AI, Erramuzpe A, Kent JD, Goncalves M, DuPre
18 E, Snyder M, Oya H, Ghosh SS, Wright J, Durnez J, Poldrack RA, Gorgolewski KJ (2018) fMRIPrep: A
19 robust preprocessing pipeline for functional MRI. Nature Methods:1.

20 Esteban O, Wright J, Markiewicz CJ, Thompson WH, Goncalves M, Ciric R, Blair RW, Feingold F,
21 Rokem A, Ghosh SS, Poldrack R (2019) NiPreps: Enabling the division of labor in neuroimaging
22 beyond fMRIPrep. Open Science Framework.

23 Fair DA, Cohen AL, Dosenbach NUF, Church JA, Miezin FM, Barch DM, Raichle ME, Petersen SE,
24 Schlaggar BL (2008) The maturing architecture of the brain's default network. Proceedings of the
25 National Academy of Sciences 105:4028–4032.

26 Fair DA, Cohen AL, Power JD, Dosenbach NUF, Church JA, Miezin FM, Schlaggar BL, Petersen SE
27 (2009) Functional brain networks develop from a "local to distributed" organization. PLOS
28 Computational Biology 5:e1000381.

29 Ferrer E, McArdle JJ, Shaywitz BA, Holahan JM, Marchione K, Shaywitz SE (2007) Longitudinal
30 models of developmental dynamics between reading and cognition from childhood to adolescence.
31 Developmental Psychology 43:1460–1473.

32 Fonov V, Evans A, McKinstry R, Almli C, Collins D (2009) Unbiased nonlinear average age-
33 appropriate brain templates from birth to adulthood. NeuroImage 47, Supplement 1:S102.

34 Fortenbaugh FC, DeGutis J, Germine L, Wilmer JB, Grosso M, Russo K, Esterman M (2015)
35 Sustained Attention Across the Life Span in a Sample of 10,000: Dissociating Ability and Strategy.
36 Psychological Science 26:1497–1510.

Fortunato S (2010) Community detection in graphs. Physics Reports 486:75–174.

Fry AF, Hale S (1996) Processing Speed, Working Memory, and Fluid Intelligence: Evidence for a Developmental Cascade. Psychological Science 7:237–241.

Fuchs LS, Fuchs D, Compton DL, Powell SR, Seethaler PM, Capizzi AM, Schatschneider C, Fletcher JM (2006) The cognitive correlates of third-grade skill in arithmetic, algorithmic computation, and arithmetic word problems. Journal of Educational Psychology 98:29–43.

Gao W, Gilmore JH, Shen D, Smith JK, Zhu H, Lin W (2013) The Synchronization within and Interaction between the Default and Dorsal Attention Networks in Early Infancy. Cerebral Cortex 23:594–603.

Gao W, Zhu H, Giovanello KS, Smith JK, Shen D, Gilmore JH, Lin W (2009) Evidence on the emergence of the brain's default network from 2-week-old to 2-year-old healthy pediatric subjects. Proceedings of the National Academy of Sciences 106:6790–6795.

Gennatas ED, Avants BB, Wolf DH, Satterthwaite TD, Ruparel K, Ciric R, Hakonarson H, Gur RE, Gur RC (2017) Age-related effects and sex differences in gray matter density, volume, mass, and cortical thickness from childhood to young adulthood. The Journal of Neuroscience:3550–3516.

Gilmore JH, Knickmeyer RC, Gao W (2018) Imaging structural and functional brain development in early childhood. Nature Reviews Neuroscience 19:123.

Ginestet CE, Nichols TE, Bullmore ET, Simmons A (2011) Brain network analysis: Separating cost from topology using cost-integration. PLOS ONE 6:e21570.

Good BH, de Montjoye Y-A, Clauset A (2010) Performance of modularity maximization in practical contexts. Physical Review E 81:046106.

Gopnik A (2020) Childhood as a solution to exploreexploit tensions. Philosophical Transactions of the Royal Society B: Biological Sciences 375:20190502.

Gorgolewski K, Burns CD, Madison C, Clark D, Halchenko YO, Waskom ML, Ghosh S (2011) Nipype: A flexible, lightweight and extensible neuroimaging data processing framework in Python. Frontiers in Neuroinformatics 5:13.

Gorgolewski KJ et al. (2017) Nipy/nipype: Release 0.13.1.

Grayson DS, Fair DA (2017) Development of large-scale functional networks from birth to adulthood: A guide to the neuroimaging literature. NeuroImage 160:15–31.

Greve DN, Fischl B (2009) Accurate and robust brain image alignment using boundary-based registration. NeuroImage 48:63–72.

Gu S, Satterthwaite TD, Medaglia JD, Yang M, Gur RE, Gur RC, Bassett DS (2015) Emergence of system roles in normative neurodevelopment. Proceedings of the National Academy of Sciences 112:13681–13686.

Guimer'a R, Nunes Amaral LA (2005) Functional cartography of complex metabolic networks. Nature 433:895–900.

Hallquist MN, Hwang K, Luna B (2013) The nuisance of nuisance regression: Spectral misspecification in a common approach to resting-state fMRI preprocessing reintroduces noise and obscures functional connectivity. NeuroImage 82:208–225.

Hodel AS (2018) Rapid Infant Prefrontal Cortex Development and Sensitivity to Early Environmental Experience. Developmental review : DR 48:113–144.

Hodgson K, Poldrack RA, Curran JE, Knowles EE, Mathias S, Göring HHH, Yao N, Olvera RL, Fox PT, Almasy L, Duggirala R, Barch DM, Blangero J, Glahn DC (2017) Shared Genetic Factors Influence Head Motion During MRI and Body Mass Index. Cerebral Cortex (New York, NY: 1991) 27:5539–5546.

Houston SM, Herting MM, Sowell ER (2014) The Neurobiology of Childhood Structural Brain Development: Conception Through Adulthood. Current topics in behavioral neurosciences 16:3–17.

Jenkinson M, Bannister P, Brady M, Smith S (2002) Improved optimization for the robust and accurate linear registration and motion correction of brain images. NeuroImage 17:825–841.

Jenkinson M, Beckmann CF, Behrens TEJ, Woolrich MW, Smith SM (2012) FSL. NeuroImage 62:782–790.

Jones JS, CALM Team the, Astle D (2021) Segregation and integration of the functional connectome in neurodevelopmentally 'at risk' children. bioRxiv:2021.05.11.443579.

Kail RV, Hulme ALC (2016) Longitudinal evidence linking processing speed to the development of reasoning. Developmental Science 19:1067–1074.

Keller JB, Hedden T, Thompson TW, Anteraper SA, Gabrieli JDE, Whitfield-Gabrieli S (2015) Resting-state anticorrelations between medial and lateral prefrontal cortex: Association with working memory, aging, and individual differences. Cortex 64:271–280.

Klein A, Ghosh SS, Bao FS, Giard J, Häme Y, Stavsky E, Lee N, Rossa B, Reuter M, Neto EC, Keshavan A (2017) Mindboggling morphometry of human brains. PLOS Computational Biology 13:e1005350.

Kopp CB (1989) Regulation of distress and negative emotions: A developmental view. Developmental Psychology 25:343–354.

Kraft AW, Mitra A, Rosenthal ZP, Dosenbach NUF, Bauer AQ, Snyder AZ, Raichle ME, Culver JP, Lee J-M (2020) Electrically coupled inhibitory interneurons constrain long-range connectivity of cortical networks. NeuroImage 215:116810.

Lancy DF (2014) The anthropology of childhood: Cherubs, chattel, changelings. Cambridge University Press.

Lanczos C (1964) Evaluation of noisy data. Journal of the Society for Industrial and Applied Mathematics Series B Numerical Analysis 1:76–85.

Lenroot RK, Giedd JN (2006) Brain development in children and adolescents: Insights from anatomical magnetic resonance imaging. Neuroscience & Biobehavioral Reviews 30:718–729.

Leonard J, Flournoy J, Lewis-de los Angeles CP, Whitaker K (2017) How much motion is too much motion? Determining motion thresholds by sample size for reproducibility in developmental resting-state MRI. Research Ideas and Outcomes 3:e12569.

Li G, Lin W, Gilmore JH, Shen D (2015) Spatial patterns, longitudinal development, and hemispheric asymmetries of cortical thickness in infants from birth to 2 years of age. Journal of Neuroscience 35:9150–9162.

Li G, Nie J, Wang L, Shi F, Lin W, Gilmore JH, Shen D (2013) Mapping Region-Specific Longitudinal Cortical Surface Expansion from Birth to 2 Years of Age. Cerebral Cortex (New York, NY) 23:2724–2733.

Lopez KC, Kandala S, Marek S, Barch DM (2019) Development of Network Topology and Functional Connectivity of the Prefrontal Cortex. Cerebral Cortex:bhz255.

Mackey AP, Miller Singley AT, Wendelken C, Bunge SA (2015) Characterizing behavioral and brain changes associated with practicing reasoning skills. PLoS ONE 10.

Maliniak D, Powers R, Walter BF (2013) The gender citation gap in international relations. International Organization 67:889–922.

Marek S et al. (2019) Identifying Reproducible Individual Differences in Childhood Functional Brain Networks: An ABCD Study. Developmental Cognitive Neuroscience:100706.

Marek S, Hwang K, Foran W, Hallquist MN, Luna B (2015) The contribution of network organization and integration to the development of cognitive control. PLOS Biology 13:e1002328.

Meyer ML, Lieberman MD (2018) Why People Are Always Thinking about Themselves: Medial Prefrontal Cortex Activity during Rest Primes Self-referential Processing. Journal of Cognitive Neuroscience 30:714–721.

Mitchell SM, Lange S, Brus H (2013) Gendered citation patterns in international relations journals. International Studies Perspectives 14:485–492.

Morgan SE, White SR, Bullmore ET, V'ertes PE (2018) A Network Neuroscience Approach to Typical and Atypical Brain Development. Biological Psychiatry: Cognitive Neuroscience and Neuroimaging 3:754–766.

Muckli L, Petro LS (2013) Network interactions: Non-geniculate input to V1. Current Opinion in Neurobiology 23:195–201.

Newman MEJ (2006) Modularity and community structure in networks. Proceedings of the National Academy of Sciences 103:8577–8582.

Nolden S, Brod G, Meyer A-K, Fandakova Y, Shing YL (2021) Neural Correlates of Successful Memory Encoding in Kindergarten and Early Elementary School Children: Longitudinal Trends and Effects of Schooling. Cerebral Cortex 31:3764–3779.

Owen AM, McMillan KM, Laird AR, Bullmore E (2005) N-back working memory paradigm: A meta-analysis of normative functional neuroimaging studies. Human Brain Mapping 25:46–59.

Pagani LS, Bri'ere FN, Janosz M (2017) Fluid reasoning skills at the high school transition predict subsequent dropout. Intelligence 62:48–53.

Parelman JM, Dor'e BP, Cooper N, O'Donnell MB, Chan H-Y, Falk EB (2021) Overlapping Functional Representations of Self- and Other-Related Thought are Separable Through Multivoxel Pattern Classification. Cerebral Cortex.

Parkes L, Fulcher B, Yücel M, Fornito A (2018) An evaluation of the efficacy, reliability, and sensitivity of motion correction strategies for resting-state functional MRI. NeuroImage 171:415–436.

Porter MA, Onnela J-P, Mucha PJ (2009) Communities in networks. Notices of the AMS 56:1082–1097.

Power JD, Barnes KA, Snyder AZ, Schlaggar BL, Petersen SE (2012) Spurious but systematic correlations in functional connectivity MRI networks arise from subject motion. NeuroImage 59:2142–2154.

Power JD, Mitra A, Laumann TO, Snyder AZ, Schlaggar BL, Petersen SE (2014a) Methods to detect, characterize, and remove motion artifact in resting state fMRI. NeuroImage 84:320–341.

Power JD, Mitra A, Laumann TO, Snyder AZ, Schlaggar BL, Petersen SE (2014b) Methods to detect, characterize, and remove motion artifact in resting state fMRI. NeuroImage 84:320–341.

Prado J, Chadha A, Booth JR (2011) The Brain Network for Deductive Reasoning: A Quantitative Meta-analysis of 28 Neuroimaging Studies. Journal of Cognitive Neuroscience 23:3483–3497.

Qi T, Schaadt G, Friederici AD (2021) Associated functional network development and language abilities in children. NeuroImage 242:118452.

R Core Team (2013) R: A language and environment for statistical computing. R Foundation for Statistical Computing, Vienna, Austria.

Raznahan A, Shaw P, Lalonde F, Stockman M, Wallace GL, Greenstein D, Clasen L, Gogtay N, Giedd JN (2011) How Does Your Cortex Grow? The Journal of Neuroscience 31:7174–7177.

Reynolds JE, Grohs MN, Dewey D, Lebel C (2019) Global and regional white matter development in early childhood. NeuroImage 196:49–58.

Risk BB, Murden RJ, Wu J, Nebel MB, Venkataraman A, Zhang Z, Qiu D (2021) Which multiband factor should you choose for your resting-state fMRI study? NeuroImage 234:117965.

Rohr CS, Arora A, Cho IYK, Katlariwala P, Dimond D, Dewey D, Bray S (2018) Functional network integration and attention skills in young children. Developmental Cognitive Neuroscience 30:200–211.

Rohr CS, Vinette SA, Parsons KAL, Cho IYK, Dimond D, Benischek A, Lebel C, Dewey D, Bray S (2017) Functional Connectivity of the Dorsal Attention Network Predicts Selective Attention in 4 year-old Girls. Cerebral Cortex 27:4350–4360.

Rubinov M, Sporns O (2010) Complex network measures of brain connectivity: Uses and interpretations. NeuroImage 52:1059–1069.

Rubinov M, Sporns O (2011) Weight-conserving characterization of complex functional brain networks. NeuroImage 56:2068–2079.

Sameroff AJ, Haith MM eds. (1996) The five to seven year shift: The age of reason and responsibility. Chicago, IL, US: University of Chicago Press.

Santarnecchi E, Galli G, Polizzotto NR, Rossi A, Rossi S (2014) Efficiency of weak brain connections support general cognitive functioning. Hum Brain Mapp 35:4566–4582.

Satterthwaite TD, Elliott MA, Gerraty RT, Ruparel K, Loughead J, Calkins ME, Eickhoff SB, Hakonarson H, Gur RC, Gur RE, Wolf DH (2013a) An improved framework for confound regression and filtering for control of motion artifact in the preprocessing of resting-state functional connectivity data. NeuroImage 64:240–256.

Satterthwaite TD, Shinohara RT, Wolf DH, Hopson RD, Elliott MA, Vandekar SN, Ruparel K, Calkins ME, Roalf DR, Gennatas ED, Jackson C, Erus G, Prabhakaran K, Davatzikos C, Detre JA, Hakonarson H, Gur RC, Gur RE (2014) Impact of puberty on the evolution of cerebral perfusion during adolescence. Proceedings of the National Academy of Sciences 111:8643–8648.

Satterthwaite TD, Wolf DH, Ruparel K, Erus G, Elliott MA, Eickhoff SB, Gennatas ED, Jackson C, Prabhakaran K, Smith A, Hakonarson H, Verma R, Davatzikos C, Gur RE, Gur RC (2013b) Heterogeneous impact of motion on fundamental patterns of developmental changes in functional connectivity during youth. NeuroImage 83:45–57.

Schaefer A, Kong R, Gordon EM, Laumann TO, Zuo X-N, Holmes AJ, Eickhoff SB, Yeo BTT (2018) Local-Global Parcellation of the Human Cerebral Cortex from Intrinsic Functional Connectivity MRI. Cerebral Cortex 28:3095–3114.

Schäfer T, Ecker C (2020) Fsbrain: An R package for the visualization of structural neuroimaging data. bioRxiv:2020.09.18.302935.

Scheipl F, Greven S, Küchenhoff H (2008) Size and power of tests for a zero random effect variance or polynomial regression in additive and linear mixed models. Computational Statistics and Data Analysis 52:3283–3299.

Smallwood J, Bernhardt BC, Leech R, Bzdok D, Jefferies E, Margulies DS (2021) The default mode network in cognition: A topographical perspective. Nature Reviews Neuroscience 22:503–513.

Sood G, Laohaprapanon S (2018) Predicting race and ethnicity from the sequence of characters in a name. arXiv preprint arXiv:180502109 Available at: https://arxiv.org/abs/1805.02109.

Souli'eres I, Dawson M, Samson F, Barbeau EB, Sahyoun CP, Strangman GE, Zeffiro TA, Mottron L (2009) Enhanced visual processing contributes to matrix reasoning in autism. Human Brain Mapping 30:4082–4107.

Stiles J, Jernigan TL (2010) The basics of brain development. Neuropsychology Review 20:327–348.

Sydnor VJ, Larsen B, Bassett DS, Alexander-Bloch A, Fair DA, Liston C, Mackey AP, Milham MP, Pines A, Roalf DR, Seidlitz J, Xu T, Raznahan A, Satterthwaite TD (2021) Neurodevelopment of the association cortices: Patterns, mechanisms, and implications for psychopathology. Neuron 0.

Teich EG, Kim JZ, Lynn CW, Simon SC, Klishin AA, Szymula KP, Srivastava P, Bassett LC, Zurn P, Dworkin JD, Bassett DS (2021) Citation inequity and gendered citation practices in contemporary physics. arXiv:211209047 [physics] Available at: https://arxiv.org/abs/2112.09047.

Thomason ME (2020) Development of Brain Networks In Utero: Relevance for Common Neural Disorders. Biological Psychiatry 88:40–50.

Thomason ME, Brown JA, Dassanayake MT, Shastri R, Marusak HA, Hernandez-Andrade E, Yeo L, Mody S, Berman S, Hassan SS, Romero R (2014) Intrinsic functional brain architecture derived from graph theoretical analysis in the human fetus. PLOS ONE 9:e94423.

Thompson-Schill SL, Ramscar M, Chrysikou EG (2009) Cognition without control: When a little frontal lobe goes a long way. Current directions in psychological science 18:259–263.

Tisdall MD, Hess AT, Reuter M, Meintjes EM, Fischl B, van der Kouwe AJW (2012) Volumetric navigators (vNavs) for prospective motion correction and selective reacquisition in neuroanatomical MRI. Magnetic Resonance in Medicine 68:389.

Tooley UA, Bassett DS, Mackey AP (2021) Environmental influences on the pace of brain development. Nature Reviews Neuroscience:1–13.

Turk E, van den Heuvel MI, Benders MJ, de Heus R, Franx A, Manning JH, Hect JL, Hernandez-Andrade E, Hassan SS, Romero R, Kahn RS, Thomason ME, van den Heuvel MP (2019) Functional Connectome of the Fetal Brain. Journal of Neuroscience 39:9716–9724.

Tustison NJ, Avants BB, Cook PA, Zheng Y, Egan A, Yushkevich PA, Gee JC (2010) N4ITK: Improved N3 bias correction. IEEE Transactions on Medical Imaging 29:1310–1320.

Van Wijk BCM, Stam CJ, Daffertshofer A (2010) Comparing brain networks of different size and connectivity density using graph theory. PLOS ONE 5:e13701.

Vendetti MS, Bunge SA (2014) Evolutionary and Developmental Changes in the Lateral Frontoparietal Network: A Little Goes a Long Way for Higher-Level Cognition. Neuron 84:906–917.

1 Volkow ND, Gordon JA, Freund MP (2020) The Healthy Brain and Child Development Study on
2 Opioid Exposure, COVID-19, and Health Disparities. JAMA Psychiatry.

3 Wang X, Dworkin JD, Zhou D, Stiso J, Falk EB, Bassett DS, Zurn P, Lydon-Staley DM (2021)
4 Gendered Citation Practices in the Field of Communication. Annals of the International
5 Communication Association 45:134–153.

6 Wechsler D, Corporation P (2012) WPPSI-IV: Wechsler preschool and primary scale of intelligence
7 – fourth edition. Bloomington, MN: Pearson, Psychological Corporation.

8 Wechsler D, Pearson Education I, Psychological Corporation (2014) WISC-V: Wechsler Intelligence
9 Scale for Children. San Antonio, TX: NCS Pearson, Inc. : PsychCorp.

10 Weimer AA, Warnell KR, Ettekal I, Cartwright KB, Guajardo NR, Liew J (2021) Correlates and
11 antecedents of theory of mind development during middle childhood and adolescence: An
12 integrated model. Developmental Review 59:100945.

13 Wellman HM (2014) Making minds: How theory of mind develops. Oxford University Press.

14 Wendelken C, Ferrer E, Whitaker KJ, Bunge SA (2016) Fronto-Parietal Network Reconfiguration
15 Supports the Development of Reasoning Ability. Cerebral Cortex 26:2178–2190.

16 Wertheim J, Ragni M (2018) The Neural Correlates of Relational Reasoning: A Meta-analysis of 47
17 Functional Magnetic Resonance Studies. Journal of Cognitive Neuroscience 30:1734–1748.

18 Whitaker KJ et al. (2016) Adolescence is associated with genomically patterned consolidation of
19 the hubs of the human brain connectome. Proceedings of the National Academy of Sciences
20 113:9105–9110.

21 Whitaker KJ, Vendetti MS, Wendelken C, Bunge SA (2018) Neuroscientific insights into the
22 development of analogical reasoning. Developmental Science 21:e12531.

23 Wierenga LM, Langen M, Oranje B, Durston S (2014) Unique developmental trajectories of cortical
24 thickness and surface area. NeuroImage 87:120–126.

25 Wig GS (2017) Segregated systems of human brain networks. Trends in Cognitive Sciences
26 21:981–996.

27 Wood SN (2011) Fast stable restricted maximum likelihood and marginal likelihood estimation of
28 semiparametric generalized linear models. Journal of the Royal Statistical Society: Series B
29 (Statistical Methodology) 73:3–36.

30 Xia Y et al. (2022) Development of functional connectome gradients during childhood and
31 adolescence. Science Bulletin.

32 Xu J, Wickramarathne TL, Chawla NV (2016a) Representing higher-order dependencies in
33 networks. Science Advances 2:e1600028.

Xu T, Cullen KR, Mueller B, Schreiner MW, Lim KO, Schulz SC, Parhi KK (2016b) Network analysis of functional brain connectivity in borderline personality disorder using resting-state fMRI. NeuroImage Clinical 11:302–315.

Yan C-G, Craddock RC, Zuo X-N, Zang Y-F, Milham MP (2013) Standardizing the intrinsic brain: Towards robust measurement of inter-individual variation in 1000 functional connectomes. NeuroImage 80:246–262.

Yeo BTT, Krienen FM, Sepulcre J, Sabuncu MR, Lashkari D, Hollinshead M, Roffman JL, Smoller JW, Zöllei L, Polimeni JR, Fischl B, Liu H, Buckner RL (2011) The organization of the human cerebral cortex estimated by intrinsic functional connectivity. Journal of Neurophysiology 106:1125–1165.

Zalesky A, Fornito A, Bullmore E (2012) On the use of correlation as a measure of network connectivity. NeuroImage 60:2096–2106.

Zhang B, Horvath S (2005) A general framework for weighted gene co-expression network analysis. Statistical Applications in Genetics and Molecular Biology 4:17.

Zhang Y, Brady M, Smith S (2001) Segmentation of brain MR images through a hidden Markov random field model and the expectation-maximization algorithm. IEEE Transactions on Medical Imaging 20:45–57.

Zhou D, Cornblath EJ, Stiso J, Teich EG, Dworkin JD, Blevins AS, Bassett DS (2020) Gender Diversity Statement and Code Notebook v1.0.

Zimmermann J, Griffiths JD, McIntosh AR (2018) Unique Mapping of Structural and Functional Connectivity on Cognition. Journal of Neuroscience 38:9658–9667.